DOI: 10.1002/chem.200600678

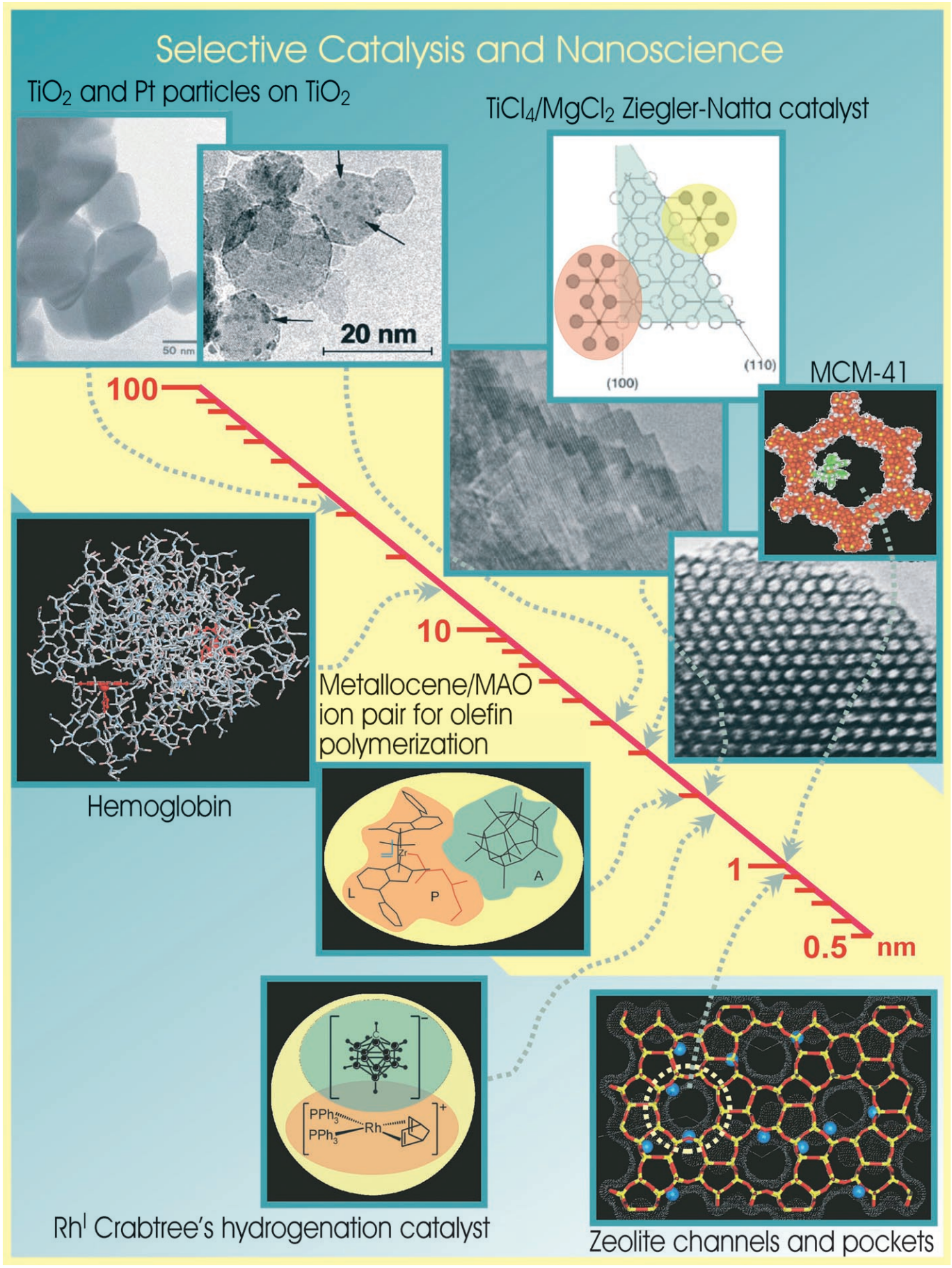

# Selective Catalysis and Nanoscience: An Inseparable Pair

**Adriano Zecchina,* Elena Groppo, and Silvia Bordiga[a]**

**Abstract:** Selective catalysts can be considered as nanomachines designed to perform the synthesis of molecules with high reaction activity and high selectivity. These properties arise from a precise control of the structure of the active sites, of the three-dimensional environment and of their relationship. In both homogeneous and heterogeneous catalysts the active site three-dimensional environment ensemble is always a complex structure resembling the tuneable structure of enzymes, which are the most efficient catalysts optimized by nature over billions of years. To illustrate this concept the structure of a few homogeneous and heterogeneous catalysts for alkenes hydrogenation and for olefin polymerization are chosen and discussed as examples.

**Keywords:** asymmetric catalysis · hydrogenation · nanotechnology · polymerization

## What Controls Activity and Selectivity of Chemical Reactions?

In solution and in the gas phase there are often many possible reactions (and hence many possible products) and the reaction outcome depends essentially on three factors: i) thermodynamic, which governs the equilibrium between reactants and products; ii) kinetic, associated to the activation barriers, on which depend the relative lifetimes of different intermediate species; and iii) statistic, which determines the probability that the reactant species can find the right pathway into the reaction medium to be transformed into a suitable product.[1] The adoption of catalysts as a mean to lower the energetic barriers associated with product formation is the usual way to reach the equilibrium in a reasonable time. The situation is even more complex because the chemical transformation of only specific targets is required, that is, a high chemical selectivity. These specific targets can be one molecule in a mixture of chemical substances or, perhaps even more difficult, one specific site in a molecule characterized by several reactive sites.

The following question thus arises: how molecules, which are complex objects with dimensions usually lower than 1 nm, can be forced to march and interact in a desired direction in a completely disorganized and chaotic environment, like a solution or a gas phase and in presence of other molecules whose access to the catalytic centre should be avoided? The answer is selective catalysis in all its forms, that is, product-, stereo-/enantio- and shape-selective. Following this line, a selective catalyst can be defined as an organized assembly of atoms and molecules, governing not only the activation barrier and the lifetime of different intermediate species (i.e., kinetic), but also the paths of the reacting molecules (i.e., statistic), eventually specifically selected from a complex mixture. It is evident that a portion of matter having these properties has at least supra- or super-supramolecular dimension and shape definitely larger than that of reactants and hence not smaller than 1 nm. Systems of this type fit the definition of nanomaterials.[2]

## The Enzymes' Lesson

In order to understand which elements determine the catalyst activity and selectivity it is useful to observe enzymes, that are the most efficient catalysts optimized by nature over billions of years. The reactions catalyzed by enzymes, in fact, take place with a reasonable speed, at room temperature and atmospheric pressure, without the formation of undesired products. One of the most important features of an enzyme core is that the activated complex is stabilized to a larger extent than the enzyme–substrate complex itself. In other words, enzymes can be considered complementary in

[a] Prof. A. Zecchina, Dr. E. Groppo, Prof. Dr. S. Bordiga
Department of Inorganic, Physical and Materials Chemistry
NIS (Nanostructured Interfaces and Surfaces) Centre of Excellence and INSTM Centro di Riferimento
University of Torino
Via P. Giuria 7, 10125 Turin (Italy)
Fax: (+39) 011-6707855
E-mail: adriano.zecchina@unito.it

  

structure to the transition state of the reaction they catalyze. The tremendously high efficiency and selectivity of the enzymes have always driven chemists to create synthetic catalytic systems that approach a similar superior activity and selectivity. By simplifying, several enzymes are characterized by a metallic site (the heart of the enzyme, where the chemical reaction occurs, responsible of product, stereo- or enantioselectivity) hosted inside channels of a complex and flexible structure originated from the assembly of one or more proteic macromolecules. The metal ions can be reached only by such reagents which are characterized by the right steric properties to enter, and the right properties to interact and diffuse inside the proteic channels. The presence of a flexible channel structure is the key factor for selectivity, by avoiding the access of all undesired molecules and protecting the active site in a not discriminate way (shape selectivity). It is thus evident that enzymes display simultaneously several types of selectivity (product-, stereo-/enantio- and shape-) and that all these properties are at the origin of their structural complexity.

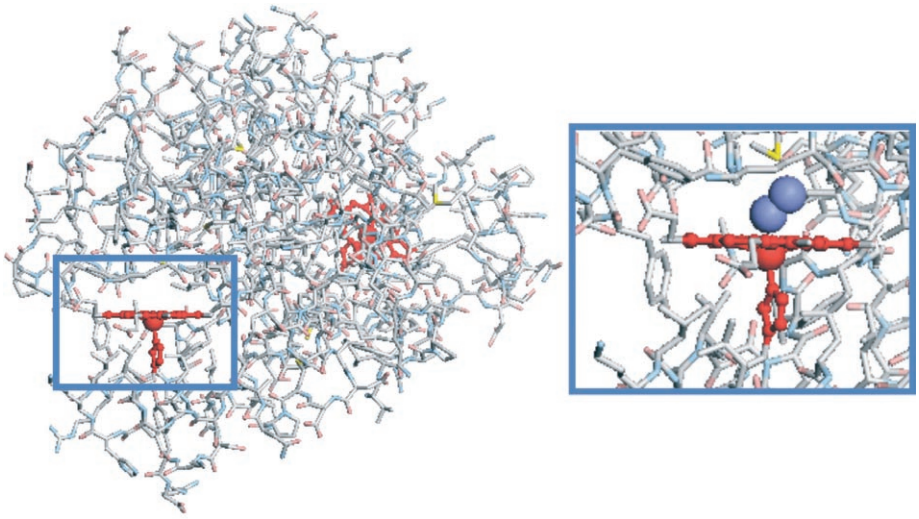

Figure 1. Structure of hemoglobin. The prosthetic groups containing the $Fe^{2+}$ cation are given in red; inset: magnification of the $Fe^{2+}(O_2)$ complex ($O_2$ in blue, prosthetic group in red) formed inside a pocket.[3]

An example of this type is hemoglobin (Figure 1). The active site is a $Fe^{2+}$ cation of a prosthetic group (red atoms in Figure 1), hosted inside a proteic structure which guarantees that the $Fe^{2+}$ cation can be reached by $O_2$ only from one direction. A $Fe^{2+}(O_2)$ complex is formed inside a pocket and is protected by the proteic framework from further dimerization (see inset in Figure 1).[3] The same concepts also apply to methane monooxygenase, which selectively oxidizes methane to methanol even in the presence of other hydrocarbons with weaker C–H bonds.[4] This specificity arises, on one side, from the product selective character of the catalytic site which is disfavoring further oxidation of methanol and, on the other side, from a sieve-like phenomenon that hampers the access of molecules bigger than methane to the active site of the enzyme. Besides size and shape, enzymes can confer specificity by means of non-covalent interactions that orient the substrate in a particular manner. As an example, in desaturated fatty acids a functional group within the active site anchors the carboxylate end of a fatty acid and thus achieve dehydrogenation at two specific carbon atoms.[5]

The lesson derived from these simple cases is that, to fulfill the requirements of product-, stereo-/enantio- and shape-selectivity, the active portion of the majority of enzymes is a combination of a metal centre, different and complex ligands in the first coordination sphere and a three-dimensional environment.

The general architecture of an enzyme has been the key of inspiration for the development of artificial supramolecular catalytic systems. To be an efficient enzyme mimic, the designed artificial selective catalysts need to possess a complex, sophisticated and tuneable structure with size in the 1–1.5 nm range, the parts of which are designed to decrease the activation barrier (central core) and to selectively recognize and bind a desired substrate, which in the next step has to be converted at a catalytic centre in its direct proximity (surrounding framework). Finally, the substrate should be able to release the converted substrate and have the ability to be regenerated. In this sense, there are clear correlations between enzymatic, homogeneous and heterogeneous catalysis.[6–8] The flexibility of the structure is necessary in all three cases for the catalytic reaction to occur efficiently, and these dynamic complex structural changes may occur at the active sites or far away the active sites, but nevertheless influencing the lifetime of reaction intermediates.

## Aim of this Paper

Before starting a detailed discussion of few specific examples, it is useful to recall that several publications have already been written on "nano-" and "selective" catalysis. Figure 2 shows that, in the last ten years, the number of scientific publications characterized by the keywords "select*" and "catal*" has more than doubled. More impressive is the growth in the number of scientific publication related to "nano*" and "catal*" (increased by more than 16 times). This trend reflects the general nano-"mania" which affects all different fields of science, and is nicely testified by the title of the National Science Foundation Workshop on catalysis in 2003: "Future directions in catalysis: structures that function on the nanoscale". The overall guiding theme and grand challenge that emerged from the NSF Workshop was

  

the control of the composition and structure of catalytic materials over length scales from 1 nm to 1 μm to provide catalytic materials that accurately and efficiently control reaction pathways. The term nanocatalysis is far from being a novelty in the scientific community. Several review articles appeared recently, showing that catalysis research is strongly linked to nanoscience.[6,9–14] The vast majority of the works cited in these review articles are related to heterogeneous catalysts based on metal nanoparticles or nanoporous systems, as we will briefly summarize in the following, without the ambition to be exhaustive on the topic.

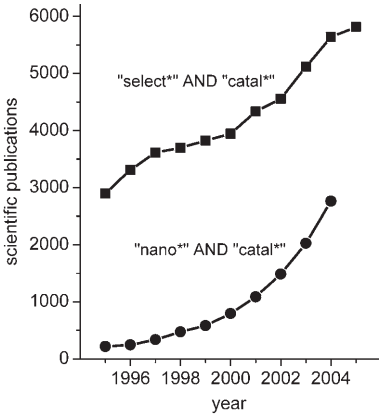


Figure 2. Publication output, in the 1995–2005 period, using the keywords depicted. Data taken from ISI Science Citation Index.

According to the concepts briefly reported above, selective nanocatalysis can be defined as the science of synthesis and in situ characterization of the ensembles of atoms with supramolecular tailored size displaying catalytic properties, with the scope of tuning with high precision[15] their activity and selectivity. A great number of examples could be reported to this end, and thousands of pages are not sufficient to exhaustively cover all the fields. However, the present work has a different ambition in order to fulfill the two following goals: The first one is to give a concise description of a selection of heterogeneous catalysts currently in use, showing that the dimensions of the relevant portions of the catalysts are always in the 1–100 nm range, and that they can be properly understood as nanomachines for the chemical manipulation of molecules to perform high precision[15] selective synthesis. The concept that the relevant portion of the catalysts can be comprised of either pockets and cavities in nanostructured materials containing chemically active centers, or a portion of the surface, in which the catalytic site is inserted. The second goal is to show that the concept of nanoscience can be applied also to artificial homogeneous catalysts that contain active sites, which are generally considered as "single-sites" having a "molecular" dimension. From the analysis of few examples extensively investigated, it will be demonstrated that, even if the dimension of what is generally considered the "active site" is smaller than 1 nm and no nanometric cavities are present to guide the selectivity, their catalytic performances arise from a precise control of the structure of the active sites, of the three-dimensional environment and of their relationship. From this analysis it can be concluded that, when the structure of the active site (including the first- and second-coordination sphere), the structure of the substrate coordinated to the active site and the structure of the surroundings (including charged counterions and solvent) are simultaneously considered, the resulting "object" fits the definition of nanomaterials and that, subsequently, selective catalysis is based on nanotechnology. In this sense, most of the homogeneous catalysts also belong to the supramolecular area of chemistry.

On the basis of these considerations, it is inferred that the distinction between heterogeneous and homogeneous selective (high precision) catalysts is vanishing.

## Positioning Heterogeneous and Homogeneous Catalysts in the 1–100 nm Scale

Figure 3 reports the length-scale of interest for nanoscience and nanotechnologies (from 100 nm down to 1 nm). In this representation some examples of catalytic systems (both homogeneous and heterogeneous) are provocatively put together along a sequence which is roughly following the dimension of the ensemble of atoms responsible for the activity and selectivity. In this section, we will first briefly discuss some of them, prevalently heterogeneous or with cage-like structure, and then we will devote a detailed discussion to two categories of systems which are among the deepest investigated from a structural and mechanistic point of view: the selective catalysts for olefin hydrogenation and the olefin polymerization catalysts.

**The nanoporous and cage-like materials**: The first examples of catalytic systems positioned in the length scale of Figure 3 are two zeolitic systems (MOR and MFI zeolites), which are here chosen because they are certainly among the best defined shape-selective heterogeneous catalysts produced so far. The catalytically relevant portion of these systems (green circle in Figure 3) is assumed to be represented by the portion of the framework constituted by the cavity, where the active centers (either Brönsted or Lewis sites or transition-metal ions or clusters) are located and where catalytic events take place, and by the minimum portion of framework surrounding it. The minimum portion of matter, designed to guide the interaction of reactants and/or the outcome of products, has always dimensions in the 1–1.5 nm range. The choice of this minimum portion is quite arbitrary since the three-dimensional organization of the channels and their hydrophobic or hydrophilic character are also playing a role in determining the final selectivity. The size of the minimum portion of matter increases moving towards MCM-41 based catalysts, because they are characterized by channels with 3–7 nm radius, which are dimensions never reached by zeolites.

  

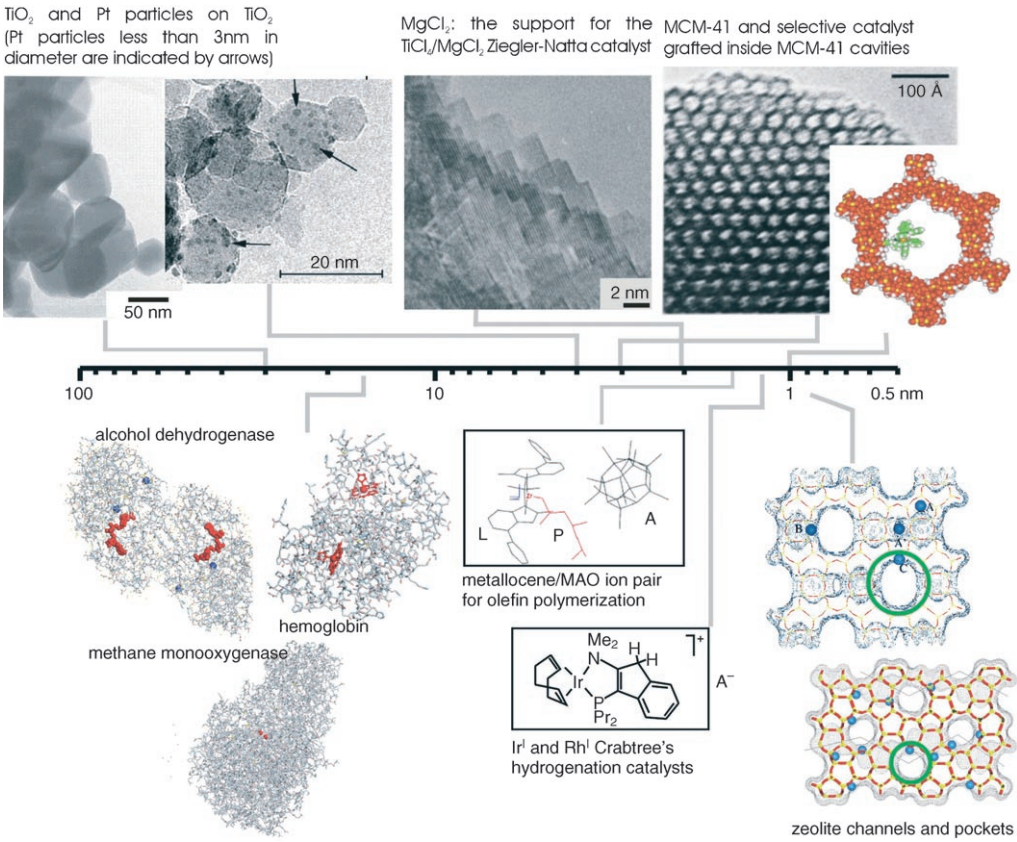


Figure 3. A few examples of selective catalysts of interest for nanoscience and nanotechnology (from 100 nm down to the atomic scale) according to their length.

The shape-selectivity concept, which originates from the field of enzymatic catalysts, has first been proposed by Paul Weisz and Frilette[16] in 1960. Several examples of shape-selective reactions can be found in a number of reviews.[17–21] Today the concept of "shape selectivity" is the basis for at least 17 commercial processes with annual hydrocarbon throughputs in more than 70 million metric tons year.[22]

The widely accepted and applicable principles exploiting shape selectivity in molecular sieves are the following.[22] i) Reactant shape selectivity distinguishes between competing reactants on the basis of size exclusion at the pore mouth. The classical example is the exclusion of multiply branched paraffins in the selective catalytic dewaxing in ZSM-5.[22,23] ii) Product shape selectivity occurs when the pore diameter discriminates between products exiting the pores on the basis of the size of the product molecules. An example is the selective disproportionation of toluene to produce *para*-xylene.[24] iii) Transition-state selectivity refers to reactions where the geometry of the cage around the active sites imposes steric constraints on the transition state. Useful examples include the inhibition of coke formation within ZSM-5 (MFI topology) crystals in the cracking of paraffins within the MFI pores.[25]

In many cases it is difficult to discriminate between the different types of shape selectivity that act in a specific process where the behavior of a catalyst is based on a combination of several factors. An outstanding example is the Ti-based molecular sieve TS-1 (see Figure 4a), where both transition state and product shape selectivities are considered to be relevant. In this case, the selectivity is dictated by the combination of isolated $Ti^{IV}$ species of well defined structure (blue balls in Figure 4a),[26] hosted in the MFI framework (red and yellow sticks in Figure 4a) and acting as hydrophilic "single site", and of channels of appropriate dimension and hydrophobic properties.[27] The combination of these two factors results in an ensemble of nanometric dimensions, where the Ti centers can be reached only by reagents of the right size and appropriate hydrophilic/hydrophobic character.[28,29] For this reason TS-1 is an election catalyst for the selective oxidation of organic substrate using hydrogen peroxide as the oxidizing agent.[30–32] In particular we can cite phenol hydroxylation, olefin epoxidation, alkane oxidation, oxidation of ammonia to hydroxylamine, conversion of secondary amines to dialkylhydroxylamines, conversion of secondary alcohols to ketones and cyclohexanone ammoximation. Figure 4 reports the phenol hydroxylation reaction, showing that the *para*- and *ortho*-isomers are exclusively obtained inside the channels of TS-1.

Similarly, Ti-based molecular sieves ETS-10[33–36] display a good selectivity in photocatalytic reactions, allowing the preferential degradation of only one given component from a mixture and overcoming the absence of selectivity which

  

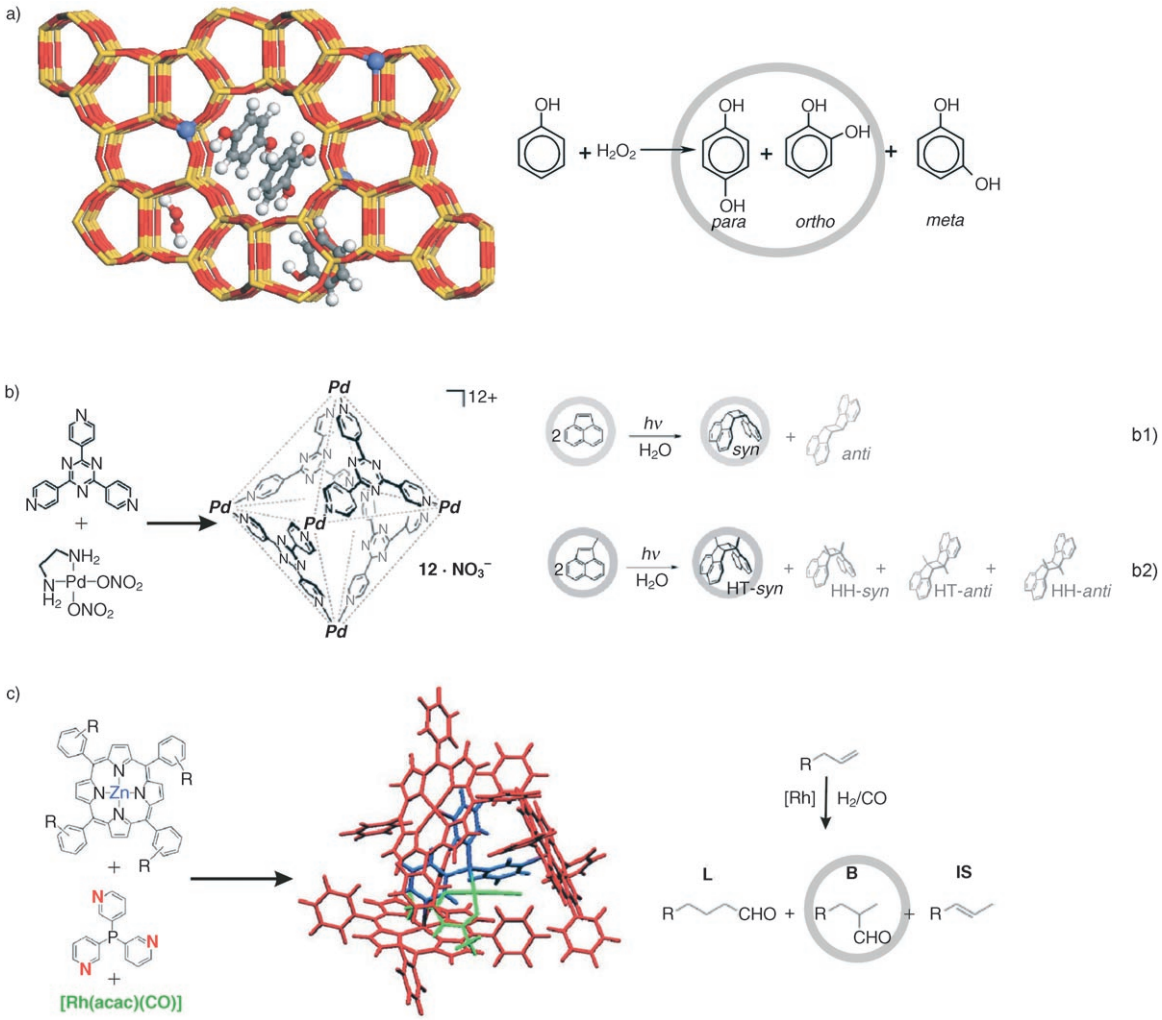


Figure 4. a) Schematic representation of a portion of TS-1 viewed along the [010] direction. The reactants (phenol and $H_2O_2$) and the products (*para* and *ortho* isomers) are represented with sticks and balls, while the zeolitic framework is represented by sticks (O and Si in red and yellow, respectively). $Ti^{IV}$ species are shown as small blue balls. b) Schematic representation of the metallocapsule obtained from the self-assembly process of four tris(*para*-pyridyl)triazine ligands and six Pd complexes. On the right the reaction schemes of the photodimerization of acenaphtylene into the *syn*-dimer (b1) and the [2+2] photodimerization of 1-methylacenaphthylene, which almost exclusively afforded the head-to-tail *syn*-isomer (b2) are reported. Adapted from *Chem. Rev.* **2005**, *105*, 1445–1489.[50] Copyright 2005 American Chemical Society. c) Formation of an encapsulated rhodium catalyst (green) by self-assembly of zinc(II) tetraphenylporphyrin as building block (red) and tris(*meta*-pyridyl)phosphine as templated ligand (blue). Right: reaction scheme of Rh-catalyzed hydroformylation of alkenes leading to linear (L), branched (B) aldehydes and isomerized (IS) olefins. Modified from ref. [15].

characterizes $TiO_2$, the classical Ti-based photocatalyst. The combination of a wide band-gap semiconducting oxide[37–40] with a three-dimensional 12-membered ring microporous framework offers many potential advantages in photocatalysis, such as excellent diffusion of reactant molecules, trapping and, in particular, shape selectivity. As a high selectivity toward the photodegradation of large aromatic molecules has been observed, it has been concluded that molecules entering the pore system were protected from photodegradation, which occurred on the external surface on specific defects. The ETS-10 system thus displays a peculiar inverse shape selectivity.[33,35,36]

In some cases, the shape-selecting cavities can be molecularly self-assembled by reactions of multitopic ligands with metal ions in solution. By adjusting the size and geometry of the organic ligand as well as the coordination preference of the metal species, one can, in principle, control the size and shape of the formed pores in the resulting frameworks, and thus the catalytic activity and selectivity.[41–50] When enantiopure chiral ligands are self-assembled with catalytically active metal ions, a homochiral metal-organic polymer is obtained, where the concept of shape-selectivity is coupled with that of stereo- or enantioselectivity. The systems thus obtained are potentially applicable as new type of heterogeneous chiral catalysts for asymmetric transformations.[51] In fact, since the stereochemical features of the chiral ligands are retained in the coordination polymers by virtue of the mild synthesis, the chiral ligand would spontaneously form a

  

chiral environment inside the cavities or on the surface of the solids for enantioselective control of the reaction, and the metal ion may act as the catalytically active centre.[52–54]

Fujita and co-workers[46] reported the synthesis of well defined cages by multicomponent transition metal-mediated self-assembly processes for the use as reaction chambers for several types of bi- and multimolecular reactions. The building blocks of these highly symmetrical metallo-capsules are simply triangular heterocyclic ligands and square-planar Pd and Pt complexes. As an example, the coordination cages reported in Figure 4b presents an inner compartment with a volume of about 500 $Å^3$, which is capable of encapsulating a variety of neutral organic molecules in aqueous environment. It has been used as a reaction chamber for the bimolecular [2+2] photodimerization of bulky olefins.[55] Upon irradiation of acenaphthylene in the presence of the metallo-capsula in water, the *syn*-dimer is formed exclusively in a yield > 98% (see reaction scheme b1 in Figure 4b). The presence of the cage appeared to be essential for the reaction to occur and, in addition, for achieving the high stereoselectivity. The cage also turned out to be a catalyst with high regioselectivity, as was evidenced by the [2+2] photodimerization of 1-methylacenaphthylene, which almost exclusively afforded the head-to-tail *syn*-isomer in a yield > 98% (see reaction scheme b2 in Figure 4b). In the absence of the cage, no reaction occurred at all.

Finally, Figure 4c reports the structure of an encapsulated rhodium catalyst obtained by self-assembly of tris(*meta*-pyridyl)phosphine and zinc(II) tetraphenylporphyrin.[15] Compared with the nonencapsulated form, this catalyst shows unprecedented high selectivity in the rhodium-catalyzed hydroformylation of internal alkenes (see Figure 4c, right), forming predominantly one of the branched aldehydes. In analogy to enzymes and zeolites, the cavity formed around the active site is of crucial importance. Likely, it reduces the rotation possibilities required for the hydride migration to the coordinated alkene.

**The supported nanoparticles**: Moving towards higher dimensions in the length scale reported in Figure 3, supported metals for selective hydrogenation reactions are represented (see upper left part), where the active particles present a diameter of ≈20 nm. Particles ranging in size from 1 to 100 nm exhibit physical and chemical properties that are intermediate between the atomic and molecular size regimes on the one hand, and the macroscopic bulk on the other.[56] The activity and selectivity of supported metal nanoparticles are strictly connected with the particle size, not only because the surface area of nanocrystals increases markedly with the decrease in size, but also because their surface structure and electronic properties change greatly in the 1–100 nm size range. It is well known that for small particles the electronic energy levels are not continuous as in bulk materials, but discrete, being the spacing between electronic energy levels strongly dependent upon the surface-to-volume ratio and the shape of the particle.[56–58] As a consequence, if electron donation or acceptance to and from reacting molecules is an important elementary step in the investigated catalytic reaction, this process should be strongly dependent on metal particle size and shape.[14,56,59–61]

This is the case of Au, which was considered inactive from a catalytic point of view for a long time, but which reveals a completely different behavior when nanometric dimensions are considered. For example, Au nanocrystals supported on titania surface show a marked size-effect in their catalytic ability for CO oxidation reaction at ambient conditions.[62,63] The activity of the Au particles is very sensitive to their size; only particles in the range of 2 to 3 nm are active.[63] Similarly, Ag nanocrystals have the capability to dissociate $O_2$ to atomic oxygen species, while on bulk Ag the adsorbed oxygen species at 80 K is predominantly $O_2^-$.[64] Small Cu and Pd nanoparticles are able to retain adsorbed CO up to much higher temperature if compared to the bulk metals;[65,66] very small Ni nanoparticles are even able to dissociate CO at 300 K forming carbidic species on the particle surface.[67,68] The activation energy for CO dissociation changes with the increasing size of the Ni particles, a pattern that affects the performance of Ni nanoparticles in Fischer–Tropsch synthesis of hydrocarbons from synthesis gas.

Finally, $TiO_2$-based photocatalysts are represented in the left-upper side of Figure 3. These systems have a definitely larger shape. In fact, although in these systems the catalytic events occur at surface specific sites (TiOH), the whole microcrystals (with dimensions around 50 nm) participate in the photocatalytic reactions, as they behave as antennas for light harvesting and for high yield electron-hole transport from bulk to surface, where photocatalysis takes place.[36] The nanoscience view is further reinforced when the presence of dyes or other species participating in the photoprocess are considered.[69–75]

**Selective catalysts for olefin hydrogenation and polymerization**: In the central part of the length scale reported in Figure 3, the catalysts for olefin hydrogenation (central bottom) and for olefin polymerization (central top) are reported. The choice of these case studies is dictated by the fact that the involved active structures are among the most widely characterized in the modern literature. Furthermore, olefin hydrogenations and polymerizations are among the few examples of chemical reactions catalyzed by both homogeneous and heterogeneous catalysts, where the maximum effort has been made both to elucidate the structure of the active site and the catalytic mechanism. For this reason, the olefin hydrogenation and polymerization catalysts become the starting points for a realistic discussion on the common aspects characterizing homogeneous and heterogeneous catalysis.

The following sections will be devoted to a detailed discussion on the role played by the solvent, by the ligands and by the cocatalyst/counterion in determining the catalytic properties of their active sites, in terms of both activity and selectivity. The common guideline is the recognition of the importance of the nanometric environment in influencing the catalytic properties of the system, which is the first step

  

in the rational manipulation of a more efficient catalyst. This concept is extremely innovative, especially for the heterogeneous catalysts, for which the active sites are in general considered in terms of well defined structures of molecular dimensions.

## Selective Catalysts for Olefin Hydrogenation

### Homogeneous cationic Rh and Ir catalysts for alkenes hydrogenation

Several types of homogeneous catalysts exist which are able to hydrogenate alkenes, in general characterized by several free coordination sites, different potential coordination numbers for a given oxidation state and different oxidation states.[76] Briefly, they include: i) the Ziegler-type systems, formed from transition-metal species activated with alkyl–lithium or aluminum compounds;[77,78] ii) the Wilkinson [$RhCl(PPh_3)_3$] catalyst and its derived systems;[79–85] and iii) the Osborn–Schrock and Crabtree catalysts and their modifications, based on $Rh^I$ and $Ir^I$ complexes.[76,86–88] The first two classes of catalysts are only effective for hydrogenations of less hindered mono- and disubstituted alkenes. Conversely, the systems belonging to the third class are more interesting, because they mediate the hydrogenation of hindered, even tri- and tetrasubstituted, alkenes, a fact which opens the way toward the synthesis of enantioselective products. As it will be shown in the following, this property arises from the possibility to vary in a wide range the constituents of the systems, that is, the selectivity of these catalysts is a property depending from all the nanometric environment.

The Osborn–Schrock and Crabtree catalysts and their modifications are complex structures, schematically composed of a cationic square-planar $Rh^I$ or $Ir^I$ procatalyst, bearing a cyclic diene and two monodentate or one bidentate P- or N-ligands (see Scheme 1, orange sphere). Since these catalysts are based on cationic metal fragments, they are always paired with an anionic counterion $A^-$, green sphere in Scheme 1. They represent, therefore, a good example of systems where the cation–counteranion interaction is extremely important (for a complete review on the role of ion-pairing effects in organometallic chemistry see ref. [89]). The correct choice of the counteranion of the ligands and also of the solvent (yellow sphere in Scheme 1) has important consequences on the catalytic activity and selectivity of these systems, as it will discussed in the following. It is evident that, when all these structural factors, including the solvation sphere, are considered, these systems have a size in the 1.0–1.5 nm range. Furthermore, since most of these components are bonded through non-covalent bonding interactions—and when the coordinated olefin is considered—these systems can be properly classified as supramolecular objects. Although all cited factors are not operating independently, we will discuss them separately for clarity.

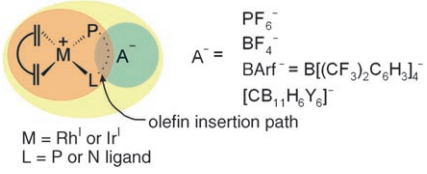


Scheme 1. The relevant portion of matter characterizing the Osborn–Schrock and Crabtree catalysts for olefin hydrogenation. The cationic centre and its ligands, the cocatalyst/counterion and the solvent are represented with orange, green and yellow spheres respectively.

**The solvent effect**: The hydrogenation reaction on Osborn–Schrock and Crabtree catalysts occurs through the oxidative addition of molecular $H_2$ (with the consequent removal of the diene ligand, step i→iii in Scheme 2), followed by the coordination of the alkene (step iii→iv in Scheme 2).[76] Solvent (S) coordination to the metal site is required to allow solvent-separated ion-pair formation and thus to stabilize the cationic reaction intermediates. Furthermore, the catalytic activation of these catalysts requires dissociation of a solvent ligand before the alkene substrate can gain access to the active site (step iii→iv in Scheme 2). It is thus not a surprise that the coordinating nature of the solvent plays an important role in determining the activity of the system (solvent effect). It has been demonstrated that cationic $Rh^I$ and $Ir^I$ systems are more active in non-coordinating solvents (such as dichloromethane or chloroform) than in coordinating solvents (such as acetone or alcohols).[76,88]

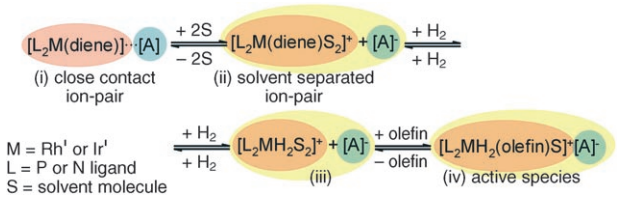


Scheme 2. Successive steps in the hydrogenation reaction on Osborn–Schrock and Crabtree catalysts (M = metal centre, L = ligands; S = solvent molecule, A = counterion). The cationic centre and its ligands, the cocatalyst/counterion and the solvent are represented with orange, green and yellow spheres respectively.

**The role of the counteranion ($A^-$)**: Another factor which plays an important role in determining the activity of cationic $Ir^I$ and $Rh^I$ hydrogenation systems is the coordinating behavior of their counteranions ($A^-$ in Schemes 1 and 2). An enhancement in activity comes from the combination of two factors: 1) the low coordinating character of the counteranion (i.e., vacant site availability) and 2) the catalyst longevity (i.e., anion stability versus anion-promoted catalyst decomposition). The importance of both these factors has been recently demonstrated for cationic $Rh^I$ Shrock–Osborn hydrogenation systems of the type [$(PPh_3)_2Rh(nbd)][A^-]$ (nbd = norbornadiene), see Scheme 3.[90,91] The use of the [*closo*-$CB_{11}H_6Br_6]^-$ carborane anion (green sphere) results

  

in a very active catalyst in the hydrogenation of internal alkenes (e.g., cyclohexenes), which is also able to hydrogenate tetrasubstituted alkenes.[90,91]

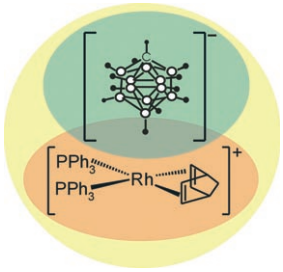


Scheme 3. The relevant components of the cationic $Rh^I$ Osborn–Schrock hydrogenation catalyst ($Rh^I$ cationic centre (orange), carborane anion (green) and solvent (yellow)).

According to the reaction mechanism shown in Scheme 2, the availability of the catalytic centre M for substrate binding increases with increasing dissociation of the complexes into solvent-separated ion pairs. Both the electronic and steric aspects of introducing particular substituents in the counteranion have a significant impact on its ion-pair behavior, and thus on the catalytic performances of the catalyst.[92] Finally, the coordinating strength of the counteranion $A^-$ is also influenced by the specificity of the interaction between the ion pair.[93,94] A kinetic study of anion effects on some $Ir^I$-mediated (green sphere in Scheme 4) hydrogenation reactions has been recently carried out for a broad range of counteranions (orange sphere in Scheme 4).[94] A strong decrease of the reaction rate was observed in the series: $BF_4^-$ > $PF_6^-$ > $B(C_6F_5)_4^-$ > $BArf^-$ > $Al(OC(CF_3)_3)_4^-$ (see Scheme 4);[94] this behavior can be explained by considering that the $BArf^-$ ion showed close contacts to the $Ir^I$ cation, while the $PF_6^-$ showed specific interactions with the ligand (see arrow in the orange sphere of Scheme 4).[93,94]

**The role of the ligands (L)**: Thus far we have discussed the role of solvent and counterion in determining the activity and selectivity of homogeneous catalysts for alkene hydrogenation. Now we move to consider the ligand coordination sphere of the $Rh^I$ and $Ir^I$ centre. The ligands properties affect not only the activity of the catalyst in terms of reaction rate, but also in terms of selectivity and/or enantioselectivity. As an example, the $Ir^I$ cationic complexes of the type reported in Scheme 4 (orange sphere) has a coordination environment similar to that of the Crabtree systems (i.e., a cationic Ir centre with a phosphine and a pyridine as the ligands). However, it is not only extremely active in the hydrogenation of tri- and tetrasubstituted alkenes, but it is also one of the rare catalysts which shows a high enantioselectivity towards unfunctionalized olefins. Unfunctionalized olefins are particularly difficult substrates because, in general, a polar group adjacent to the C=C bond, which coordinates with the metal centre, is required for high catalyst activity and enantioselectivity. For this reason, there are only few examples of highly enantioselective hydrogenations of olefins devoid of a coordinating group.[95–98] The cationic $Ir^I$ complexes of the type reported in Scheme 4 are able to hydrogenate unfunctionalized olefins with high enantioselectivity with a very low loading (0.1–0.5 mol%). The ligand design has been revealed a key factor in the optimization of enantioselectivity for this catalyst. A systematic study of the influence of the Ar and R ligands, in fact, led to the conclusion that the most efficient catalyst is characterized by Ar = Tol and R = *t*Bu, which gave high conversions and yields excellent *ee* values for a number of trisubstituted olefins.

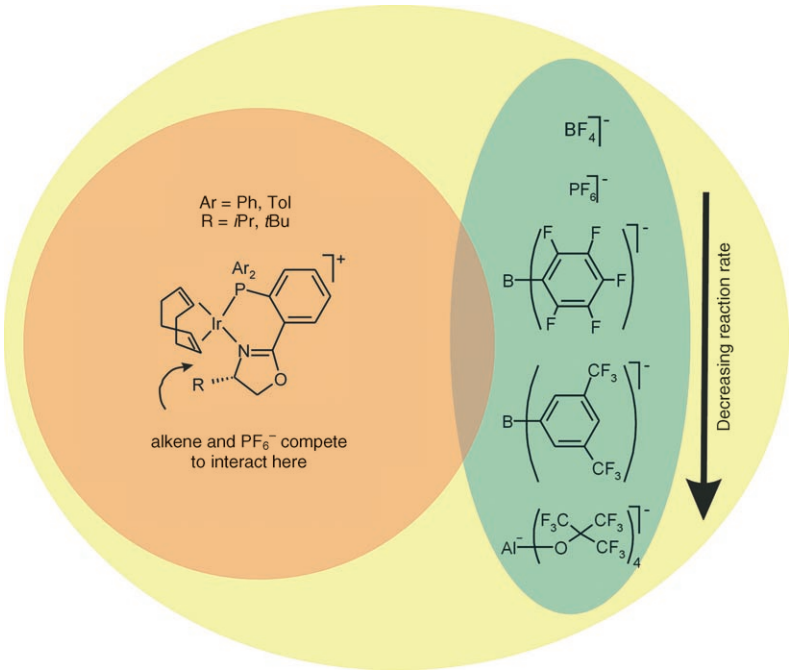


Scheme 4. Main constituents of an $Ir^I$-based hydrogenation catalyst and effect of the counterion on the hydrogenation reaction. The cationic centre and its ligands, the cocatalyst/counterion and the solvent are represented with orange, green and yellow spheres respectively.

Of course, enantioselectivity is governed not only by the ligands, but also by the counteranions, as observed for cationic $Rh^I$–phosphine fragments coordinated to sulfonate anions.[83] A significant counteranion effect has also been reported in cationic $Ir^I$ phosphanodihydrooxazole-based hydrogenation systems: moving from $PF_6^-$- to $BArf^-$-type counterions has a positive effect on the conversion, enantiomeric excess, and catalyst stability in the high-pressure (50 bar) hydrogenation of sterically very-hindered stilbene derivatives, although the exact role of the counterion in the catalytic cycle remains unresolved.[99]

  

From the discussion made until now, it is evident that the whole catalyst ensemble constituted by the cationic moiety, the anionic counterparts and the solvent, contribute to the enantioselectivity. It is becoming clear that the chemical operations by this system are complex. This conclusion is not substantially modified when the most recent investigations on these systems concerning the discovery of zwitterionic relatives of $Ir^I$-based hydrogenation catalysts are considered, which are capable of mediating the hydrogenation of alkenes under mild conditions in a wider range of solvents.[100] These systems are characterized by a formally cationic Ir centre, counterbalanced by an indenide anion built into the backbone of a supporting (P,N) ligand, as in the neutral complex of the type reported in Figure 5b. The formally charge-separated species such as that reported in Figure 5b combine the appealing catalytic activity of the more traditional catalysts (Figure 5a) with the desirable solubility properties associated with neutral complexes. The development of hydrocarbon-soluble zwitterionic $Ir^I$ catalysts of this type is also of particular interest for the following two principal reasons: i) they provide a general means of circumventing the use of environmentally harmful chlorocarbon solvents and ii) by employing a relatively inert, low-coordinating hydrocarbon as the reaction medium for hydrogenations, the catalyst life, reaction rate, and selectivity can be improved.

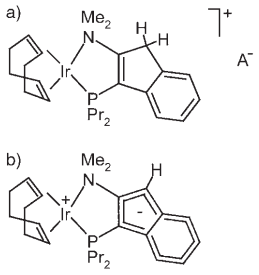


Figure 5. Cationic a), and zwitterionic b) forms of an $Ir^I$-based hydrogenation catalyst.

**Modifications of the Rh and Ir hydrogenation catalysts—towards heterogeneous systems**: Very recently, chiral $Rh^I$–diphosphine complexes have been incorporated into self-assembled thiolate monolayers (SAMs) on gold colloids with formation of catalytic spheres of about 3.0 nm in diameter. Catalysts of this type are of extreme interest, because they combine properties of homogeneous and heterogeneous systems, as well as of enzymes. Figure 6 reports an example of these complexes, where the $Rh^I$–diphosphine end groups (orange sphere) are coupled with the corresponding counteranion ($BArf^-$, green sphere). It is clear that, once again, the size of the active catalytic site is incredibly great. The immobilized Rh catalysts proved to be active and showed virtually the same enantioselectivity as the analogous homogeneous catalyst but, in addition, offer the unique possibility to tune the catalytic properties of the metal centre simply by modifying the neighboring thiolate molecules.[101]

This example demonstrates once more that the borderline between molecular type Crabtree and Osborn catalysts and even more complex catalytic nanomachines with shape similar to that of enzymes is progressively disappearing.

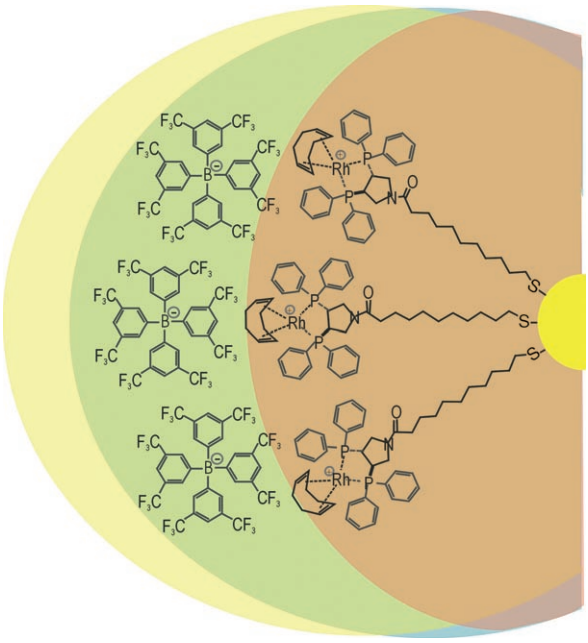


Figure 6. Example of a functionalized gold particle coated with a monolayer of thiolates (orange sphere) with chiral $Rh^I$–diphosphine end groups. The green sphere represents the corresponding counteranion ($BArf^-$), while the yellow one represents the solvent effect. Reproduced in part with permission from *J. Am. Chem. Soc.* **2005**, *127*, 8720.[101] Copyright 2005 American Chemical Society.

**Transferring enantioselectivity to heterogeneous catalysts for hydrogenation reactions**: The hydrogenation of olefins (or even more complex substrates) in heterogeneous phase is generally performed with metal supported particles (Pd, Pt). The reaction, occurring at the surface of the metal particles, is usually not selective. The olefin (or the substrate, in general) and the hydrogen molecules, in fact, are simultaneously adsorbed on the surface. Hydrogen is dissociated by the metal and then hydrogenates the olefin in the adsorbed state. As the olefin is surrounded by a multitude of mobile hydrogen atoms, the attack is not specific and hence enantioselectivity cannot be attained. The question is, therefore, how chiral recognition and enantioselectivity can be induced on a metal particle? One possibility emerges from the fact that metal catalyst particles are not perfectly symmetric structures, but contain defects such as kinks, some of which may be chiral. Such intrinsically chiral sites can be created deliberately by cutting a metal single crystal along certain high Miller index planes.[102–105] However, in the absence of additional chiral information, the amount of left- and right-handed kink sites (or other chiral structures) is equal. Hence such catalysts are racemic and do not yield enantiomeric excess.

To induce selectivity other components must be added to the pristine catalyst in a similar way to what discussed above for homogeneous systems. Also, in this case, the combination of the new components with the original metallic catalyst yields a complex nanomaterial with properties not present in the precursor. Learning from the enzymes, in

  

order to attain selectivity, it is necessary to design a specific reaction path for the olefin molecules. This can be achieved by building a three-dimensional structure on the metal surface to properly direct the olefin molecule towards the adsorbed hydrogen atoms. A possible, quite easy, but not well governed, solution can be found by covering the metal surface with nanocrystals of NaCl or other salts, which form cubic "nanobuildings". The interstices between some of the nanobuildings constitute preferential paths which can orient the olefin molecules during their interaction with the adsorbed hydrogen atoms. It is evident that the shape, dimension and location of salt buildings are key elements for the selectivity control. Simultaneously, the presence of salt buildings emerging from the metal surface changes the proportion of hydrogen species (on top, double and triply bridged) and hence contribute to the selectivity, since also the structure of adsorbed hydrogen is influential. A mixture of the two effects is likely at the base of the improved selectivity of Pd metal surfaces doped with alkaline salts.[106–111] Several authors have also proposed to preliminary modify the proportion of surface hydrogen species by employing Pd/Au (or Pt/Au) alloys, instead of the pure metal. Moreover, the use of bimetallic catalysts can be a way to increase the resistance to the particle sintering, and to change the geometry and the electronic properties of the active sites.[112–114]

When enantioselectivity is required, a chiral surface must be present. A simple and efficient approach to create a chiral surface under mild conditions is the presence of a chiral organic compound on a metal surface.[115,116] Particularly striking is the progress made in the chiral modification of supported Pt and Pd catalysts by means of cinchona alkaloids, applied in enantioselective hydrogenation of functionalized ketones and enantioselective hydrogenation of C=C bonds, respectively.[102,117–121] In these cases, an important role is not only played by the conformation and adsorption modes of cinchona alkaloid on the metallic surface (orange sphere in Figure 7), but also by the polarity of the solvent used during the reaction (yellow sphere in Figure 7).[122] Figure 7 provides a three-dimensional view of two surface conformations of cinchonidine adsorbed on Pt surface.[120] It well illustrates the crucial role of the complex three-dimensional structure of the modifier in defining the chiral space (chiral pocket).

In complete contrast to the cases discussed above, McIntosh et al.[123] recently ruled out the role of the metal surface in the enantioselective hydrogenation of isophorone to dihydroisophorone. It has been demonstrated that in the proline-directed asymmetric hydrogenation of isophorone, the catalyst surface (Pd, in this case) does not participate in the key enantio-differentiating event, which actually occurs homogeneously in the solution phase. These results seem to represent an exception with respect to the heterogeneous hydrogenation catalysts illustrated so far, where the enantioselectivity was always associated with a specific modification of the catalyst surface through the anchoring of chiral agents. In this sense, the catalyst dimension should be considered very small, and the structure of the active sites extremely simple. However, the metal catalyst does, of course, also play a role in these systems, at least in two fundamental phases because: i) it enables the initial racemic hydrogenation, and ii) it drives the kinetic resolution equilibrium step to completion, by irreversibly removing the final enantiomer by a further hydrogenation step. It is thus clear that, also in a case where the metal surface does not play a direct role in determine the enantioselectivity of a reaction, the overall catalytic properties can be described only by considering a nanometric environment.

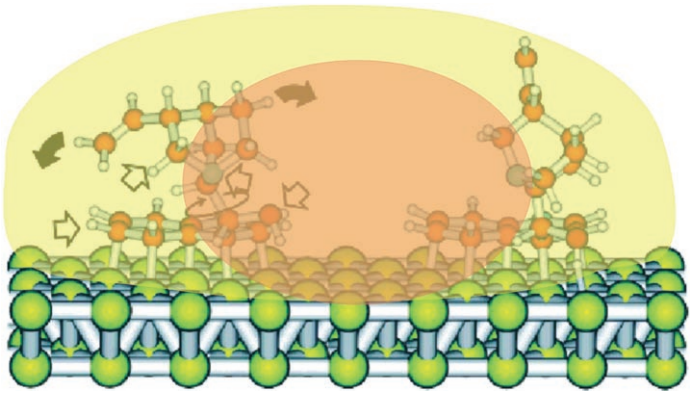

Figure 7. Surface conformations of cinchonidine on the Pt surface. The circular arrow indicates the rotation of the quinuclidine skeleton; black arrows indicate the possible rotation of the quinuclidine skeleton toward and away from the surface; open arrows indicate the elements contributing to attractive and repulsive interactions and forming the chiral pocket on the metal surface. N, O, C, H and Pt atoms are represented in blue, red, orange, white and yellow colors, respectively. The transparent orange sphere represents the size of the active site, while the yellow one represents the solvent. Reproduced in part with permission from *J. Am. Chem. Soc.* **2005**, *127*, 8467.[120] Copyright 2005 American Chemical Society.

## Olefin Polymerization Catalysts: Structure–Activity–Selectivity Relationships

Polymers produced by homo-polymerization and/or co-polymerization of small olefins, such as ethylene and propylene, are among the most widely used plastics. With the exception of the low-density polyethylene (LDPE), which is made by a high temperature/high pressure radical process, the other types of polyolefins are produced by using either homogeneous or heterogeneous catalysts operating at relatively low temperatures (353–453 K) and pressures ($<50$ bar). Basically, three main classes of olefin polymerization catalysts can be distinguished: i) the Ziegler–Natta heterogeneous catalysts,[124–130] ii) the Phillips-type heterogeneous catalysts,[131–136] and iii) the single-site homogeneous catalysts (or supported homogeneous catalysts), such as metallocene catalysts.[137,138]

Since the 1950s, most of the important polymers have been made by using catalysts with only limited control over the range of lengths of the polymer chains (low product selectivity), as well as over other structural features that govern the properties of the material. Chemists have long

  

realized that improved catalysts could offer better control over polymerization, thus making it possible to create plastic materials with physical properties specifically tuned to particular uses. Indeed, the relationship between the structure of the active sites and the catalytic activity is the core of the study in catalysis, and the rational manipulation of the catalyst structure to improve the catalytic activity is consequently the main scope of catalyst design. The $TiCl_4/MgCl_2$ Ziegler–Natta and the $Cr/SiO_2$ Phillips catalysts for olefin polymerization offer two paradigmatic examples. The difficulties encountered in the investigation and in the improvement of the properties of these catalysts mainly derive from the heterogeneity of the supports. For this reason, over the years, the modifications of catalytic activity of the systems and the subsequent properties of the produced polymers have been slowly obtained by modifying the support with promoters or by adopting different activation procedures, mainly on the basis of phenomenological observations. Despite these slow improvements, these catalysts still play a dominant role in the polymerization industry. Their permanent vitality can be explained by considering that, even if their original development was made in a "rough" way, the progressive modification of the ligand coordination sphere allowed to obtain better and better results.

Major discoveries in how to create catalysts that provide superb control over olefin oligomerization and polymerization have been made in the past two decades in the field of single-site homogeneous catalysts.[139–142] With homogeneous catalysts the two major shortcomings of traditional heterogeneous Ziegler–Natta catalysts, that is, the presence of multiple active sites and the high sensitivity to heteroatoms, can be potentially avoided. In fact, as they contain only a single active site for which ligand sphere can be properly tailored, these homogeneous catalysts provide a much finer control over the final product and open the way to the preparation of completely new polymers. However, we will demonstrate in the following that the single-site nature of these catalysts does not correspond to a simplification of the catalyst structure, which is as complex as that of the heterogeneous counterparts.

**Heterogeneous olefin polymerization catalysts**

**The Ziegler–Natta catalyst**: $TiCl_4/MgCl_2$ catalysts and their variations are today the most commonly used heterogeneous Ziegler–Natta catalysts, apart from being also the major olefin polymerization catalysts. Despite their obvious importance, many aspects of classical Ziegler–Natta catalysts are largely unknown. Important properties such as the structure of the active sites, the role of the support and the differences between the activity of the transition metal in various oxidation states are poorly understood, mostly because it is difficult to employ experimental methods to study the low concentrated active sites that exist in a relatively disordered environment.[129] Despite this, we will show that, even starting from an intrinsic heterogeneity of the system, a good stereoselectivity has been obtained by the continuous controlled increase of the complexity of the active sites, following a design which renders the difference between heterogeneous and homogeneous polymerization catalysts smaller than would have been anticipated.

The classical Ziegler–Natta catalysts are nowadays obtained by reacting $TiCl_4$ on $MgCl_2$ in presence of an alkyl aluminum compound (most commonly $AlEt_3$) as an activator. For this reason, present assessments on the structure of the active sites in the classical Ziegler–Natta catalysts generally start from the geometry of crystalline $MgCl_2$. The most widely studied surfaces are (110) and (100), which are the representative surfaces for four- and five-coordinated Mg ions, respectively.[143] The most recent results suggest that the coordination of mononuclear $TiCl_4$ is only possible on the (110) surfaces (yellow sphere in Figure 8), where Mg is four-coordinated, whereas on the (110) surface coordination of dimeric $TiCl_4$ is favored (orange sphere in Figure 8).[143–145] Notably these last sites present a chiral environment. Two different types of sites in which a $TiCl_4$ is bound to one or more uncoordinated Mg ions have been proposed in the literature, in which Ti ion is five-[146] or six-coordinated,[147] respectively.

When the catalyst is activated, the coordinated $TiCl_4$ on the different $MgCl_2$ planes creates active sites with different Lewis acidic strengths, steric hindrance and Ti oxidation states. The activation of the catalyst involves alkylation and reduction of Ti, according to the steps represented in Figure 8. In the first step, one Cl ligand at the Ti centre is exchanged for an alkyl group of the alkyl aluminum compound. In the next step, $Ti^{4+}$ is reduced to $Ti^{3+}$ by splitting off an alkyl radical. This alkyl radical is deactivated by reaction with a further alkyl radical. By these two reaction steps, a vacant site at the Ti centre is formed, which is necessary to complex and activate the ethylene molecule.

The structure of the active sites thus generated corresponds to the structure of active sites for the polymerization of olefins as postulated by Cossee and Arlman, and it is in line with the Rideal mechanism for heterogeneous catalytic processes.[148–150] According to the Rideal mechanism, the first step of the reaction at the surface of a heterogeneous catalyst is the coordination of a monomer molecule into a vacant position of the metal site carrying an alkyl chain via a d–π interaction. The second step is a migratory insertion reaction into the metal−alkyl bond that extends the growing alkyl chain by one monomer unit, thereby regenerating the vacant coordination site at the metal centre. Figure 8 illustrates this mechanism, taking as an example the polymerization of ethylene: in each insertion step of the activated monomer into the Ti−C bond, a new Ti−C bond is formed and the vacant site is regenerated for complexation of the next monomer molecule. The crystallinity of the support is keeping the heterogeneity of sites at a low level, thus ensuring a good control of molecular weight distribution.

However, despite the crystallinity of the support, the $TiCl_4/MgCl_2$ Ziegler–Natta catalysts are not very stereospecific in the propene polymerization. This has stimulated a great effort to enhance the selectivity by introducing suita-

  

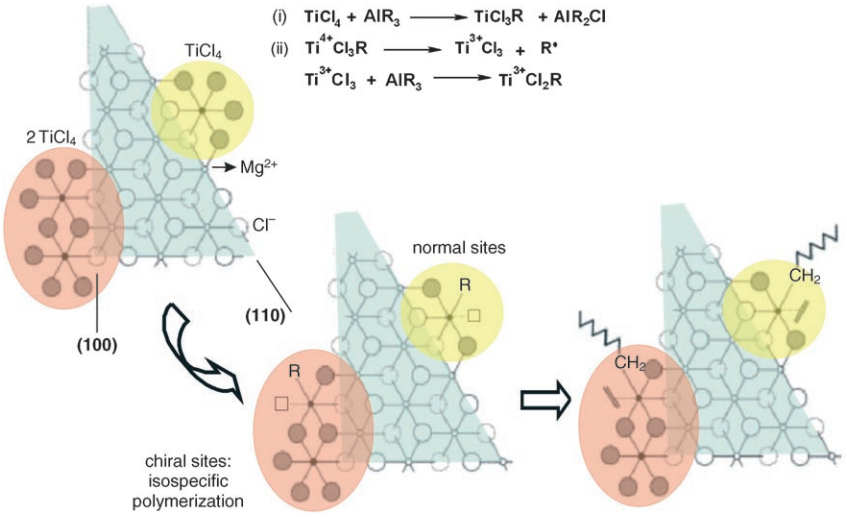


Figure 8. From left to right, schematic representation of the formation of the active centers on the surface of the Ziegler–Natta $TiCl_4/MgCl_2$ catalysts and of the subsequent ethylene polymerization reaction. Both the phenomena occur at the surface of $MgCl_2$. The bulk $MgCl_2$ is evidenced by the light blue triangle; normal and chiral active sites are represented in orange and yellow, respectively. Adapted from ref. [129].

ble modifiers. The goal has been achieved by introduction of "internal" and "external" electron donors.[151] The amount of electron donors is an adjustable parameter in the polymerization, which is used to control the stereospecificity of the catalyst.[152–158]

Among other effects, the function of the internal donor (diesters) in $MgCl_2$-supported catalysts is to stabilize small primary crystallites of $MgCl_2$. Another possible function of the internal donor is that, due to the higher acidity of the coordination sites on the (110) face, preferential coordination of the donor on these sites will avoid the formation of Ti species having poor selectivity (yellow sphere in Figure 8), and favor the activity of dimeric sites of the (100) faces (orange sphere in Figure 8), whose environment is chiral, a necessary condition for isospecific polymerization.

The requirement for an external donor (alkoxysilane) when using catalysts which contain an ester as an internal donor is due to the fact that, when the catalyst is brought into contact with the co-catalyst, a large proportion of the internal donor is lost as a result of alkylation and/or complexation reactions. In the absence of an external donor, this leads to poor stereoselectivity due to increased mobility of the Ti species on the catalyst surface. Conversely, when the external donor is present, contact of the catalyst components leads to replacement of the internal donor by the external donor.[157]

Although the catalyst modifications described thus far are based more on a hypothesis than on detailed knowledge of the sites structure, the obtained results are highly satisfactory. From the concise above-mentioned discussion, one conclusion is emerging: the active site of a selective Ziegler–Natta catalyst has a complex nanometric structure where several components (crystallinity, face index and promoters) play a concerted role.

**The Phillips catalyst**: The $Cr/SiO_2$ Phillips catalysts,[132] responsible for producing more than one third of all the PE in the world,[136,159,160] are commonly obtained by reacting a Cr precursor (inorganic or organometallic, for example, $H_2CrO_4$ etc.) and surface silanols with formation of grafted $Cr^{VI}$ species. A typical catalyst contains about 0.5–1.0 wt % Cr.[134,136] The $Cr^{VI}$ precursors are then reduced by $C_2H_4$ (industrial process)[134] or by CO (model laboratory process),[134–136,161–163] with formation of anchored $Cr^{II}$ species where the silica particle acts as a complex multidentate ligand. The reduced species react further with $C_2H_4$, leading to direct formation of polymer chains anchored to the Cr centers. Notwithstanding the numerous efforts, some questions still remain controversial, in a similar way to what occurs for the Ziegler–Natta system: i) the exact structure of the Cr active sites;[136] ii) the number of actually active Cr sites on the silica surface;[164] and iii) the initiation mechanism.[136,165] In particular, a direct relation between the structure of the Cr sites and the catalytic activity has recently been subjected to a detailed investigation.[172]

Concerning point i), the detailed structure of the anchored chromium species, both in the oxidized and in the reduced form of the catalyst, has been a strong point of discussion in the literature and several spectroscopic techniques (UV/Vis, DRS, IR, Raman, XAS, XPS, etc.) have been employed to solve the problem.[135,136] Concerning the reduced form of the catalyst, the common opinion is that the structure of the anchored $Cr^{II}$ ions is extremely heterogeneous, because the $Cr^{II}$ ions can be linked to the silica surface in several ways thus reflecting the high heterogeneity of the amorphous support.[134,136] IR spectroscopy of probe molecules has been preferentially used to discriminate among the different $Cr^{II}$ sites on the silica surface.[136,166–171] The conclusion arising from all of these works is that on the CO pre-reduced Phillips catalyst a distribution of $Cr^{II}$ sites is present, all active in the ethylene polymerization, but characterized by a different polymerization rate. The whole process of $Cr^{VI}$ anchoring, surface activation and successive CO reduction are represented in Figure 9b.

The catalyst activation procedure plays an important role in determining the properties of the grafted Cr sites, by contributing both on the dehydroxylation of the silica surface and on the relative distribution of the $Cr^{II}$ sites on the silica surface. It is a matter of fact that the polymerization activity of the Phillips catalyst grows with surface dehydroxylation.

  

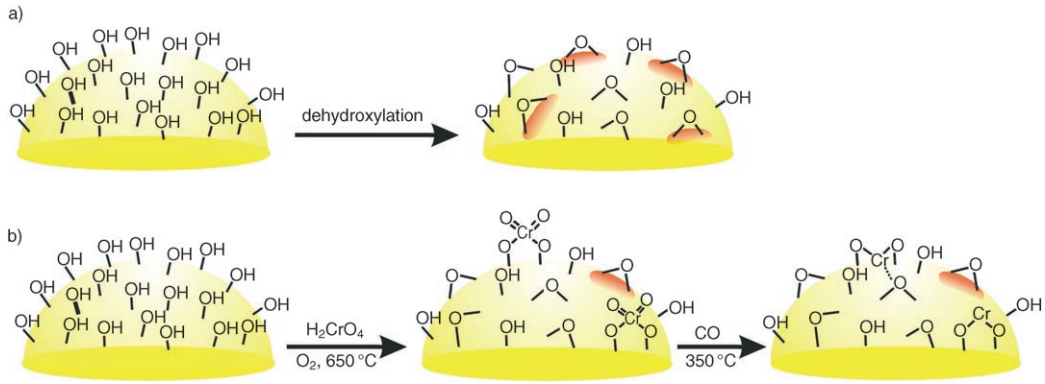


Figure 9. Schematic representation of a) the dehydroxylation process occurring on the silica surface and b) the whole process of anchoring, surface activation and CO reduction for the $Cr/SiO_2$ Phillips system. The orange patches correspond to the portions of silica surface characterized by a high strain.

As the numerous studies carried out on this system exclude the direct involvement of the hydroxyls in the catalytic centers,[162] this implies that the presence of highly dehydroxylated patches on the silica surface influences the activity of Cr active centers located on them. This effect is associated with the strain induced on the surface bonds by dehydroxylation. In other words the activity of a specific centre is modulated by changing the hydroxylation state of that part of the silica particle surface where the strain is induced. In general terms, the effect of dehydroxylation can be fully understood when the parallel process on the pure silica surface is considered. This is schematically represented in Figure 9a, where it is clear that dehydroxylation of the silica surface is accompanied by formation of ≡Si–O–Si≡ bridges where the Si–Si distance is different with respect to that of the bulk. This is accompanied by an increasing accumulation of surface strain (see orange patches in Figure 9b). The strain induced on the silica surface by thermal activation decreases when Cr sites are grafted on it (see the smaller number of orange patches in Figure 8b), because it is compensated by the counter-effect of the large $Cr^{II}$ ions which, due to their transition metal character, display a superior coordination ability towards oxygen atoms in vicinal position (see dotted line in the right part of Figure 9b).

The role of the thermal activation in influencing the strain properties of the silica surface and thus of the grafted Cr centers has been recently demonstrated by discovering that it is possible to tune the relative population of different $Cr^{II}$ sites by changing the activation conditions.[172] Roughly speaking, we can distinguish among "slow" and "fast" Cr sites, according to the speed of the polymerization reaction occurring on them. In particular, it has been found that the catalyst subjected to a thermal annealing is characterized by a lower number of "slow" $Cr^{II}$ sites which, conversely, constitute the greatest fraction of active $Cr^{II}$ on a standard system. Since the "slow" $Cr^{II}$ sites are responsible for the production of short and disordered polymeric chains, this is basically the origin of the broad molecular weight distribution, which characterizes the polyethylene obtained by the Phillips catalyst.[172] The influence of the surface activation on the properties of the resulting polymer is shown schematically in Figure 10.

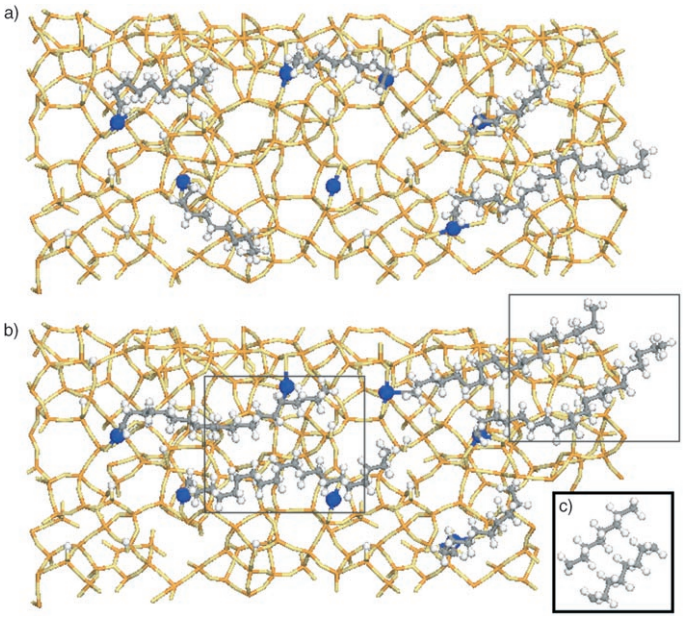


Figure 10. Qualitative representation of the surface of a standard Phillips catalysts and of the same system subjected to a thermal annealing (parts a and b, respectively) carrying some polymeric chains. The product selectivity is achieved by changing the activation conditions. Red and yellow sticks connect together silicon and oxygen atoms respectively; the big blue balls represent $Cr^{II}$ ions, while the little gray and white balls represent carbon and hydrogen atoms, respectively. Gray rectangles in part b) highlight the regions in which the polymeric chains are interacting at a distance (average C–C distance of 4.0 Å) in the same order of that characterizing crystal polyethylene (part c). Reproduced from *J. Catal.* **2005** *236*, 233,[172] with permission. Copyright 2005 by Elsevier.

In conclusion, the rational manipulation of the surface properties of the silica support indirectly influences the structure of the Cr active sites. The manipulation of the

  

giant "silica ligand" induced by thermal activation recalls the classical method of ligand modification normally used in homogeneous polymerization catalysts. By exploiting the ability to change the strain properties and the coordination state of the active sites, it is possible to tune the properties of the resulting polymer, that is, to achieve a product selectivity. Finally, from the above discussion it is also emerging that the active site is not only constituted by the Cr site and its nearest neighbors, but also by the atoms present in the surrounding dehydrated area. It is thus evident that the so-called active site has nanometric dimensions and the connection between (product) selectivity and nanoscience is clearly emerging also in this case.

**Single-site homogeneous catalysts for olefin oligomerization and polymerization**

Typically, a single-site olefin polymerization catalyst is obtained by mixing in-situ a structurally well-defined organometallic compound, usually a metallocene–dichloride complex (catalyst precursor), with an activator (or cocatalyst), generally a Lewis acid, such as methylaluminoxane (MAO) or $B(C_6F_5)_3$. In this way the active catalytic system, composed of a cationic metal species ($M^+$) and an anionic complex ($A^-$), is generated. It is now generally accepted that, in a non-polar polymerization medium, the cation and the counteranion likely form an ion pair.[89,173,174] Figure 11,

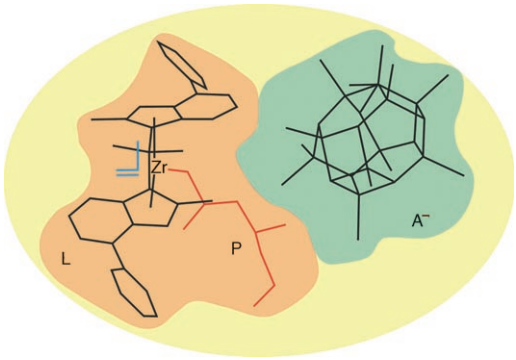


Figure 11. Model of the active site for olefin polymerization in the case of a Zr-based metallocene complex. $A^-$ denotes the MAO counteranion, P the initial polymer chain and L the organic ligand used to achieve stereocontrol and activity enhancement. The inserting propylene molecule is reported in blue. The three colored spheres define the close-contact ion pair (orange-green spheres), which reaches nanometric dimensions and the solvent (yellow sphere). Reproduced in part with permission from *Chem. Rev.* **2000**, *100*, 1435.[141] Copyright 2000 American Chemical Society.

which reports the active site model of a modern Zr-based propylene polymerization catalyst, demonstrates the molecular complexity of the question at hand. Five main components constitute the metallocene catalytic system.[141]

1) The cationic metal species (Zr in Figure 11), where the polymeric $M{-}C_nH_{2n+1}$ chain grows. As the stability of the M–C bond largely determines the activity of the catalytic centre, it is foreseen that the electronic structure of the metal centre should play a role in determining the chain length and hence the product selectivity in terms of oligomers or polymers formation.
2) The large and sterically elaborate ligand (L, the orange sphere in Figure 11) the main function of which is to tune both polymerization activity and stereocontrol. In general, the transition-metal ion bears two $\eta^5$-cyclopentadienyl ligands (which can be tethered by a bridging unit) and two σ-ligands (usually Cl atoms). The two cyclopentadienyl ligands remain attached to the metal during the polymerization (for this reason they are also referred to as "ancillary" or "spectator" ligands) and actually define the catalyst stereoselectivity and activity, as we will describe in the following. Due to their aromaticity, cyclopentadienyl anions are six-electron donors and very robust ligands. Conversely, one or both of the two σ-ligands are removed when the active catalyst is formed (see below).
3) The counterion ($A^-$, green sphere in Figure 11), which is likely present as a solvent-separated or contact ion pair, and thus is not an innocent bystander. The counterion is formed during the catalyst activation. As MAO is the most used activator, it is inferred that the $A^-$ counterion has a complex structure.
4) The coordinated olefin substrate (propylene, reported blue in Figure 11) .
5) The living polymer chain (P, reported in red in Figure 11), which is known to influence the course of the reaction both from the product selectivity (chain length) and from the stereospecific point of view.
6) The solvent (yellow sphere in Figure 11), which is tuning the cation–anion separation and hence influence the accessibility of the catalytic site to the incoming olefin.

The ensemble constituted by all these components (colored spheres in Figure 11) is characterized by nanometric dimensions. Furthermore, most of these constituents are bonded together through non-covalent and coordinative interactions. We can here verify once more that this ensemble properly belong to the supramolecular field of chemistry. By investigating one of the five components discussed above it is possible to greatly change the catalytic performances of the system in terms of activity and selectivity. With a rational choice of the metal and/or of the ligands it is possible to influence the activity and to convert a polymerization catalyst into a selective oligomerization one, or to have a stereo- or regiocontrol of the polymerization reaction. As the above-mentioned factors operate together in a concerted way, it is difficult to discuss their effect separately. In this short review we will only illustrate a few examples concerning the role of the ligand, the role of the counterion structure and of the solvent in determining the activity, the product selectivity and the stereoselectivity. A more detailed discussion of all factors, including the role of the metal cation electronic structure,[175–178] can be found in the more specialized literature.

  

**Polymerization catalysts—The role of the ligands (L) in determining the catalytic performances**: By considering the same metal centre, small changes in the type and position of the ligands can have a drastic effect on the activity of the catalyst and on the properties of the polymers. An example of the possibility to adjust various ligands with the aim of changing the performance of the catalyst is illustrated in Figure 12. Reported in Figure 12 are the top five most active Zr-based ethylene polymerization catalysts (Figure 12a) and four metallocene systems characterized by low ethylene polymerization activity (Figure 12b). The first two complexes reported in Figure 12a represent the most active metallocene dichloride complexes (under the polymerization conditions indicated) that have ever been published.[140] An explanation of their behavior may rely in steric effects: in fact, all the methyl substituents are in direct contact with the active catalyst centre, thus increasing the distance between the cationic metal centre and the anionic MAO cocatalyst. Steric effects, such as the bite angle between the two $\eta^5$-coordinated aromatic ligands or bulky substituents at these ligands, dramatically influence the catalytic performance. This is the case of the complexes reported in Figure 12.

So far we have discussed the role of ligand structure in the control of the polymer length and hence in the product selectivity of the catalyst. In order to discuss the influence of the ligand structure on the control of stereoselectivity and regioselectivity, the polypropylene (PP) case is the most suitable. In fact, to make high quality isotactic PP it should be ensured that the monomers fit into the active site in only one orientation in 99% of the time. At present, single-site metallocene catalysts are objects of increasing research particularly focusing on their stereochemical properties.[179–185] The stereoselectivity in polymerization of propylene and higher α-olefins is, to a large proportion, due to the type and position of the ligands forming the complex. This is the basis of the so-called "enantiomorphic site control", that is, it is the chirality of the coordination site that determines the stereochemistry of the polymer.[1] The steric hindrance of active centre and the electronic modification due to the π-ligands are the two essential factors that determine the catalysts performance.[179] The metallocene complexes which allow a control of the stereo- and regioselectivity of the polymerization reaction belong to the class of *ansa*-metallocenes, which consist of two indenyl ligands (Cp ligands with a fused benzene ring) that are linked by a bridge. By this means the ligand sphere can be fixed in a certain geometry providing a chiral metal centre. Propylene polymerizations with catalysts of this type indeed yield highly isotactic polymers.

The catalysts operating by site control can be divided into three main classes (see Table 1), according to the symmetry of the ligands: a) the *ansa*-$C_2$ symmetric types; b) the species with a centre of asymmetry ($C_s$ symmetry); and c) the *ansa*-$C_1$-symmetric catalysts. These three classes of catalysts are responsible for the production of isotactic (iPP), syndiotactic (sPP) and hemi-isotactic/isotactic polypropylene, respectively.[139] The key to obtain a sPP relies on a flipping of the polymer chain from one active site side to the other side during the monomer insertion: for $C_s$ symmetric catalysts the active site isomerizes if the polymer chain flips from one side to the other, whereas this does not occur in $C_2$ symmetric catalysts.[186,187] It is thus clear that an appropriate modification of the ligands constituting the catalyst precursor gives the opportunity to achieve enhanced stereocontrol, increased MW and improved catalyst productivity.

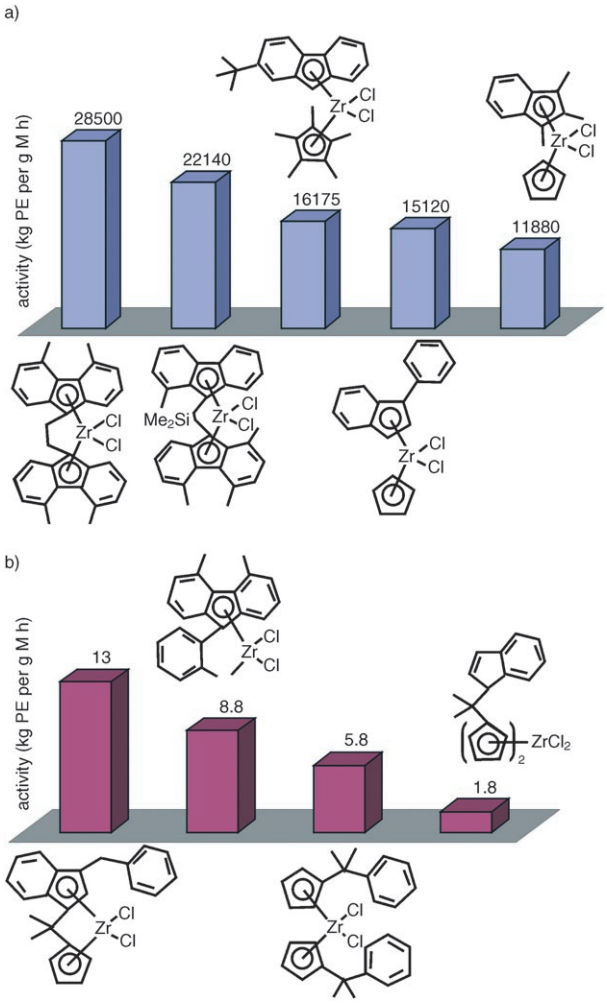


Figure 12. Examples of the influence of the ligands on the activity of Zr-based ethylene polymerization catalysts. a) Top five of the most active metallocene complexes. b) Four metallocene complexes characterized by low ethylene polymerization activity. Reactions conducted at 10–60 °C in *n*-pentane with $p_{C_2H_4} = 10.0$ bar. Adapted from *Chem. Rev.* **2000**, *100*, 1205[140]. Copyright 2000 American Chemical Society.

**Polymerization catalysts—The role of the counteranion ($A^-$) in determining the catalytic performances**: Concerning the role of the counteranion in determining the catalytic

[1] Note that every monomer insertion generates a new stereogenic centre, so that chiral induction can come also from the last unit. This is based on the so-called chain-end control mechanism, for which we refer to the more specialized literature.

  

Table 1. Prototypes of the three classes of stereospecific metallocenes catalysts, according to their symmetry.

| symmetry | $C_2$ | $C_s$ | $C_1$ |
|---|---|---|---|
| prototype | 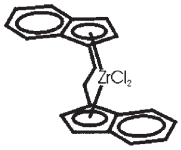 |  | 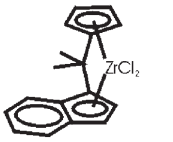 |
| polymer |  isotactic PP |  syndiotactic PP |  hemiisotactic-isotactic PP |

performances, it is worth emphasizing that, if the molecular structure of the organometallic precursors is generally well determined, conversely the complex system resulting from its reaction with the activator ($A^-$ in Figure 11) is far from being a well defined one for several reasons. The identification of: i) the structure of the counteranion, ii) the cation–anion interaction and iii) the interaction of the ion pair with the olefin, are the principal problems.[140,173] For all these regions the investigation of the active centre is a complex task.

Recently, a number of computational studies aiming to elucidate these points has emerged.[188–191] It is now accepted that the counteranion plays an important role in the polymerization process by strongly affecting the catalyst stability and activity, the stereoregularity, the average molecular weights and the branching of the resulting polymers.[173] Polymerization catalysts can be converted into oligomerization or dimerization catalysts simply by changing the counteranion. Unfortunately, due to the size of the counteranions, which is in the nm range, theoretically studies of the polymerization mechanism where the anion is incorporated involve considerable computational effort.[190,191]

As MAO is still the best co-catalyst for single-site olefin polymerization homogeneous catalysts, it is useful to devote some attention to it. MAO, usually expressed as $[\text{-Al}(CH_3)\text{O-}]_n$, is prepared by careful hydrolysis of $AlMe_3$, though its composition is far from being known. Cryoscopic, GPC, and NMR studies have shown that MAO is a mixture of different several compounds, including residual $AlMe_3$ and possibly $AlO_3$ units, in dynamic equilibrium.[192] The MAO molecular mass (i.e., the oligomerization degree n) varies over a wide range ($n = 6$–30) and depends on the preparation procedure.[190,191,193] The activity of the catalysts in olefin polymerization depends on the MAO oligomerization degree and in general increases with increasing values of $n$. A detailed study carried out by Barron and co-workers[194,195] on the hydrolysis products of $Al(t\text{Bu})_3$ might suggest that dynamic cage structures, consisting of three-coordinate oxygen and four-coordinate aluminum atoms, are more likely than linear or cyclic structures. Recent DFT calculations of Zakharov et al.[193] also found that cage structures with $n > 4$ (see Figure 13) are much more energetically stable than ring or fused ring structures. A dynamic equilibrium between different MAO cages has been proposed and the average molecular formula of a MAO oligomer was estimated to be $[\text{-Al}(CH_3)\text{O-}]_{17.23}$ at 298 K.[189–191]

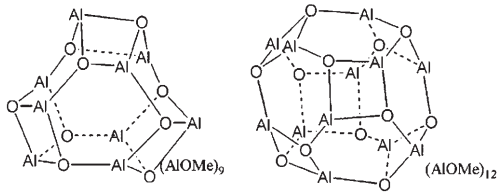


Figure 13. Most stable MAO cages structures, composed of square and hexagonal faces, according to the calculation of Zurek et al.[189]

The generally accepted mechanism of metallocene activation by MAO is shown schematically in Scheme 5 (where, for simplicity, MAO is represented in a linear form) and consists of the following steps: i) alkylation of the catalyst precursor, generally by replacing chlorides from a dichloro complex with methyl groups; ii) abstract of a $CH_3^-$ anion from the transition-metal complex, forming a monomethyl cationic species; iii) stabilization of the cationic complex, acting as a weakly coordinating counterion. The formal contact ion pair is the active catalyst.[141,173,196] The less the ion interactions, the better the catalyst's activity. Bulky ligands at the transition metal precursor can indeed keep the MAO anion at a certain distance and produce a more or less "naked" metallocene monomethyl cation. As a consequence, the activity can be increased by factors of 5 or 6.[140]

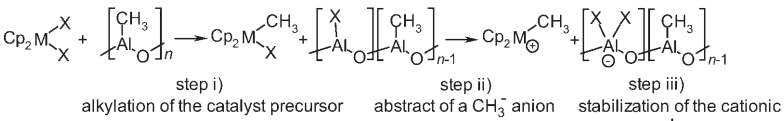


Scheme 5. Generally accepted mechanism of metallocene activation by MAO (for simplicity MAO is represented in a linear form).

Zurek et al.[189] have studied the mechanism of ethylene insertion into the metal–alkyl bond and the role of the

  

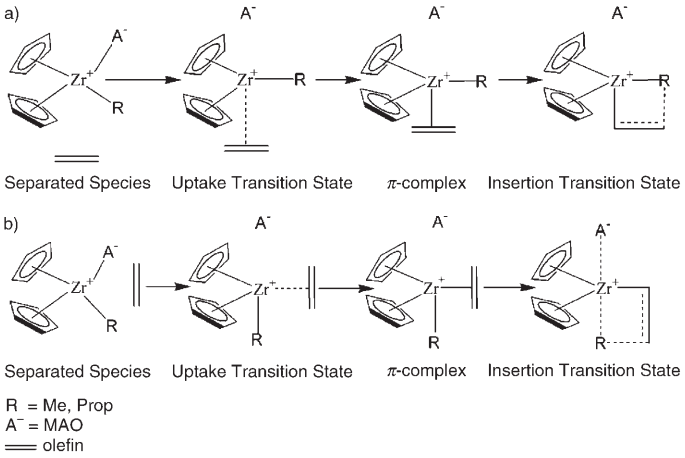


Figure 14. a) Dissociative and b) associative ethylene insertion mechanism into the Zr–R bond of an ion pair proposed in ref. [197]. The ethylene is shown approaching *trans* (a) and *cis* (b) to the μ-methyl bridge. In the dissociative mechanism a), the transition state occurs when the cation ($Zr^+$) and counteranion ($A^-$) are still separated and the Zr is four-coordinated. In the associative mechanism b), the μ-methyl bond is only slightly elongated at the transition state and the Zr is five-coordinated. Reproduced in part with permission from *Prog. Polym. Sci.* **2004**, *29*, 107.[189] Copyright 2004 Elsevier.

counterion $A^-$ from a theoretical point of view in great detail. A dissociative and an associative mechanism were considered as reported in Figure 14, parts a) and b), respectively. In both mechanisms, the cation and counteranion dissociate during the approach of the olefin to the cation, resulting in the formation of a dissociated π-complex. Next, ethylene approaches the metal–alkyl bond leading to the formation of a four-membered cyclic transition state. In the dissociative mechanism (Figure 14a), the transition state occurs when the cation and counteranion are still separated and the Zr is four-coordinated. In the associative mechanism (Figure 14b), the μ-methyl bond is only slightly elongated at the transition state and the Zr is five-coordinate.

From these schemes, it is clear that the olefin binding and the counteranion binding are two competitive reactions. The weaker the coordinating power of the anion, the higher the reactivity for a given cation. Strongly coordinating anions compete with olefins to occupy the coordination site *cis* to the polymer group, and consequently, the activity of the catalyst is reduced. As the coordination ability of the catalytic centre is tuned by the cation–anion interaction, the role of solvent in influencing the catalytic performances clearly emerges.

From all these considerations it is concluded that a polymerization catalyst is a complex structure constituted by several parts operating in a concerted way. Its definition as a nanomachine with shape in the nanometer range and design for selective synthesis of specific structures is thus well documented.

## Conclusions

Artificial catalysts displaying high activity and selectivity are complex and tuneable structures with nanometric dimensions. This concept is valid for both homogeneous and heterogeneous catalysts. Alkenes hydrogenation and olefin polymerization catalysts have been chosen as examples to illustrate that selective catalysts can be considered as nanomachines for molecule assembling, whose parts are designed to perform several functions, such as the decrease of the activation barrier, the selection of reactants and products and the stereo-/enantioselective synthesis. It is concluded that not only for the nanostructured heterogeneous selective catalysts, but also for the homogeneous catalysts, the relevant portion of the structure involved in the catalytic functions has nanometric dimension.

[1] C. Lamberti, E. Groppo, G. Spoto, S. Bordiga, A. Zecchina, *Adv. Catal.* **2007**, *51*, 1–74.
[2] J. Chorkendorff, W. Niemantsverdriet, *Concepts of modern catalysis and kinetics*, Wiley-VCH, Weinheim, **2003**.
[3] J. P. Collman, R. Boulatov, C. J. Sunderland, L. Fu, *Chem. Rev.* **2004**, *104*, 561–588.
[4] M. Merkx, D. A. Kopp, M. H. Sazinsky, J. L. Blazyk, J. Muller, S. J. Lippard, *Angew. Chem.* **2001**, *113*, 2860–2888; *Angew. Chem. Int. Ed.* **2001**, *40*, 2782–2807.
[5] B. G. Fox, K. S. Lyle, C. E. Rogge, *Acc. Chem. Res.* **2004**, *37*, 421–429.
[6] "Future Directions of Catalysis Science—Workshop": *Catal. Lett.* **2001**, *76*, 111–124.
[7] R. Mas-Balleste, L. Que, *Science* **2006**, *312*, 1885–1886.
[8] S. Das, C. D. Incarvito, R. H. Crabtree, G. W. Brudvig, *Science* **2006**, *312*, 1941–1943.
[9] G. A. Somorjai, Y. G. Borodko, *Catal. Lett.* **2001**, *76*, 1–5.
[10] A. T. Bell, *Science* **2003**, *299*, 1688–1691.
[11] J. Grunes, A. Zhu, G. A. Somorjai, *Chem. Commun.* **2003**, 2257–2260.
[12] H. J. Freund, J. Libuda, M. Baumer, T. Risse, A. Carlsson, *Chem. Rec.* **2003**, *3*, 181–200.
[13] R. Schlogl, S. B. Abd Hamid, *Angew. Chem.* **2004**, *116*, 1656–1667; *Angew. Chem. Int. Ed.* **2004**, *43*, 1628–1637.
[14] D. Astruc, F. Lu, J. R. Aranzaes, *Angew. Chem.* **2005**, *117*, 8062–8083; *Angew. Chem. Int. Ed.* **2005**, *44*, 7852–7872.
[15] M. Kuil, T. Soltner, P. van Leeuwen, J. N. H. Reek, *J. Am. Chem. Soc.* **2006**, *128*, 11344–11345.
[16] P. B. Weisz, V. J. Frilette, *J. Phys. Chem.* **1960**, *64*, 382–382.
[17] W. Hölderich, M. Hesse, F. Näumann, *Angew. Chem.* **1988**, *100*, 232–251; *Angew. Chem. Int. Ed. Engl.* **1988**, *27*, 226–246.
[18] P. B. Venuto, *Microporous Mater.* **1994**, *2*, 297–411.
[19] A. Corma, H. Garcia, *Catal. Today* **1997**, *38*, 257–308.
[20] J. C. van der Waal, H. van Bekkum, *J. Porous Mater.* **1998**, *5*, 289–303.
[21] C. Song, *Stud. Surf. Sci. Catal.* **1998**, *113*, 163–186.
[22] T. F. Degnan, *J. Catal.* **2003**, *216*, 32–46.
[23] N. Y. Chen, R. L. Gorring, H. R. Ireland, T. R. Stain, *Oil Gas J.* **1977**, *75*, 165.
[24] T. C. Tsai, S. B. Liu, I. K. Wang, *Appl. Catal. A* **1999**, *181*, 355–398.
[25] T. F. Degnan, G. K. Chitnis, P. H. Schipper, *Microporous Mesoporous Mater.* **2000**, *35–36*, 245–252.
[26] C. Lamberti, S. Bordiga, A. Zecchina, G. Artioli, G. L. Marra, G. Spanò, *J. Am. Chem. Soc.* **2001**, *123*, 2204–2212.
[27] S. Bordiga, A. Damin, F. Bonino, C. Lamberti, *Top. Organomet. Chem.* **2005**, *16*, 37–68.

  

[28] F. Bonino, A. Damin, G. Ricchiardi, M. Ricci, G. Spanò, R. D'Aloisio, A. Zecchina, C. Lamberti, C. Prestipino, S. Bordiga, *J. Phys. Chem. B* **2004**, *108*, 3573–3583.
[29] C. Prestipino, F. Bonino, A. Usseglio Nanot, A. Damin, A. Tasso, M. G. Clerici, S. Bordiga, F. D'Acapito, A. Zecchina, C. Lamberti, *ChemPhysChem* **2004**, *5*, 1799–1804.
[30] B. Notari, *Adv. Catal.* **1996**, *41*, 253.
[31] C. Perego, A. Carati, P. Ingallina, M. A. Mantegazza, G. Bellussi, *Appl. Catal. A* **2001**, *221*, 63–72.
[32] P. Ratnasamy, D. Srinivas, H. Knözinger, *Adv. Catal.* **2004**, *48*, 1–169.
[33] P. Calza, C. Paze, E. Pelizzetti, A. Zecchina, *Chem. Commun.* **2001**, 2130–2131.
[34] P. D. Southon, R. F. Howe, *Chem. Mater.* **2002**, *14*, 4209–4218.
[35] F. X. Llabres i Xamena, P. Calza, C. Lamberti, C. Prestipino, A. Damin, S. Bordiga, E. Pelizzetti, A. Zecchina, *J. Am. Chem. Soc.* **2003**, *125*, 2264–2271.
[36] S. Usseglio, P. Calza, A. Damin, C. Minero, S. Bordiga, C. Lamberti, E. Pelizzetti, A. Zecchina, *Chem. Mater.* **2006**, *18*, 3412–3424.
[37] E. Borello, C. Lamberti, S. Bordiga, A. Zecchina, C. Otero Arean, *Appl. Phys. Lett.* **1997**, *71*, 2319–2321.
[38] C. Lamberti, *Microporous Mesoporous Mater.* **1999**, *30*, 155–163.
[39] S. Bordiga, G. Turnes Palomino, A. Zecchina, G. Ranghino, E. Giamello, C. Lamberti, *J. Chem. Phys.* **2000**, *112*, 3859–3867.
[40] A. Damin, F. X. Llabres i Xamena, C. Lamberti, B. Civalleri, C. M. Zicovich-Wilson, A. Zecchina, *J. Phys. Chem. B* **2004**, *108*, 1328–1336.
[41] O. M. Yaghi, M. O'Keeffe, N. W. Ockwig, H. K. Chae, M. Eddaoudi, J. Kim, *Nature* **2003**, *423*, 705–714.
[42] S. Leininger, B. Olenyuk, P. J. Stang, *Chem. Rev.* **2000**, *100*, 853–907.
[43] R. Pinalli, V. Cristini, V. Sottili, S. Geremia, M. Campagnolo, A. Caneschi, E. Dalcanale, *J. Am. Chem. Soc.* **2004**, *126*, 6516–6517.
[44] S. R. Seidel, P. J. Stang, *Acc. Chem. Res.* **2002**, *35*, 972–983.
[45] B. J. Holliday, C. A. Mirkin, *Angew. Chem.* **2001**, *113*, 2076–2097; *Angew. Chem. Int. Ed.* **2001**, *40*, 2022–2043.
[46] M. Fujita, *Chem. Soc. Rev.* **1998**, *27*, 417–425.
[47] A. W. Kleij, J. N. H. Reek, *Chem. Eur. J.* **2006**, *12*, 4219–4227.
[48] A. Lutzen, *Angew. Chem.* **2005**, *117*, 1022–1025; *Angew. Chem. Int. Ed.* **2005**, *44*, 1000–1002.
[49] J. Rebek, *Angew. Chem.* **2005**, *117*, 2104–2115; *Angew. Chem. Int. Ed.* **2005**, *44*, 2068–2078.
[50] D. M. Vriezema, M. C. Aragones, J. Elemans, J. Cornelissen, A. E. Rowan, R. J. M. Nolte, *Chem. Rev.* **2005**, *105*, 1445–1489.
[51] J. S. Seo, D. Whang, H. Lee, S. I. Jun, J. Oh, Y. J. Jeon, K. Kim, *Nature* **2000**, *404*, 982–986.
[52] X. W. Wang, K. L. Ding, *J. Am. Chem. Soc.* **2004**, *126*, 10524–10525.
[53] L. X. Dai, *Angew. Chem.* **2004**, *116*, 5846–5850; *Angew. Chem. Int. Ed.* **2004**, *43*, 5726–5729.
[54] K. L. Ding, Z. Wang, X. W. Wang, Y. X. Liang, X. S. Wang, *Chem. Eur. J.* **2006**, *12*, 5188–5197.
[55] M. Yoshizawa, Y. Takeyama, T. Kusukawa, M. Fujita, *Angew. Chem.* **2002**, *114*, 1403–1405; *Angew. Chem. Int. Ed.* **2002**, *41*, 1347–1349.
[56] C. N. R. Rao, G. U. Kulkarni, P. J. Thomas, P. P. Edwards, *Chem. Eur. J.* **2002**, *8*, 29–35.
[57] E. A. Rohlfing, D. M. Cox, A. Kaldor, *J. Phys. Chem.* **1984**, *88*, 4497–4502.
[58] D. E. Powers, S. G. Hansen, M. E. Geusic, D. L. Michalopoulos, R. E. Smalley, *J. Chem. Phys.* **1983**, *78*, 2866–2881.
[59] D. J. Trevor, D. M. Cox, A. Kaldor, *J. Am. Chem. Soc.* **1990**, *112*, 3742–3749.
[60] B. D. Leskiw, A. W. Castleman, *Chem. Phys. Lett.* **2000**, *316*, 31–36.
[61] B. C. Gates, *J. Mol. Catal. A* **2000**, *163*, 55–65.
[62] G. C. Bond, D. T. Thompson, *Catal. Rev. Sci. Eng.* **1999**, *41*, 319–388.
[63] M. Valden, X. Lai, D. W. Goodman, *Science* **1998**, *281*, 1647–1650.
[64] C. N. R. Rao, V. Vijayakrishnan, A. K. Santra, M. W. J. Prins, *Angew. Chem.* **1992**, *104*, 1110–1112; *Angew. Chem. Int. Ed. Engl.* **1992**, *31*, 1062–1064.
[65] A. K. Santra, S. Ghosh, C. N. R. Rao, *Langmuir* **1994**, *10*, 3937–3939.
[66] E. Gillet, S. Channakhone, V. Matolin, M. Gillet, *Surf. Sci.* **1985**, *152–153*, 603–614.
[67] D. L. Doering, J. T. Dickinson, H. Poppa, *J. Catal.* **1982**, *73*, 91–103.
[68] D. L. Doering, H. Poppa, J. T. Dickinson, *J. Catal.* **1982**, *73*, 104–119.
[69] A. Z. Ruiz, H. R. Li, G. Calzaferri, *Angew. Chem.* **2006**, *118*, 5408–5413; *Angew. Chem. Int. Ed.* **2006**, *45*, 5282–5287.
[70] O. Carp, C. L. Huisman, A. Reller, *Prog. Solid State Chem.* **2004**, *32*, 33–177.
[71] J. C. Yu, Y. D. Xie, H. Y. Tang, L. Z. Zhang, H. C. Chan, J. C. Zhao, *J. Photochem. Photobiol. A* **2003**, *156*, 235–241.
[72] G. Mele, G. Ciccarella, G. Vasapollo, E. Garcia-Lopez, L. Palmisano, M. Schiavello, *Appl. Catal. B* **2002**, *38*, 309–319.
[73] M. Yang, D. W. Thompson, G. J. Meyer, *Inorg. Chem.* **2002**, *41*, 1254–1262.
[74] H. Sakai, R. Baba, K. Hashimoto, A. Fujishima, A. Heller, *J. Phys. Chem.* **1995**, *99*, 11896–11900.
[75] P. V. Kamat, *Chem. Rev.* **1993**, *93*, 267–300.
[76] "The mechanism of homogeneous hydrogenation": P. A. Chaloner, M. A. Esteruelas, F. Joo, L. A. Oro, in *Homogeneous hydrogenation* (Eds.: R. Ugo, B. R. James), Kluwer, Dordrecht, **1994**.
[77] R. Waymouth, P. Pino, *J. Am. Chem. Soc.* **1990**, *112*, 4911–4914.
[78] A. L. Rheingold, N. P. Robinson, J. Whelan, B. Bosnich, *Organometallics* **1992**, *11*, 1869–1876.
[79] M. Bowker, J. L. Gland, R. W. Joyner, Y. X. Li, M. M. Slinko, R. Whyman, *Catal. Lett.* **1994**, *25*, 293–308.
[80] M. Bartok, G. Szollosi, A. Mastalir, I. Dekany, *J. Mol. Catal. A* **1999**, *139*, 227–234.
[81] M. E. Quiroga, E. A. Cagnola, D. A. Liprandi, P. C. L'Argentiere, *J. Mol. Catal. A* **1999**, *149*, 147–152.
[82] B. Richter, A. L. Spek, G. van Koten, B. J. Deelman, *J. Am. Chem. Soc.* **2000**, *122*, 3945–3951.
[83] J. M. Buriak, J. C. Klein, D. G. Herrington, J. A. Osborn, *Chem. Eur. J.* **2000**, *6*, 139–150.
[84] C. Merckle, S. Haubrich, J. Blumel, *J. Organomet. Chem.* **2001**, *627*, 44–54.
[85] I. Bar-Nahum, R. Neumann, *Chem. Commun.* **2003**, 2690–2691.
[86] X. H. Cui, K. Burgess, *Chem. Rev.* **2005**, *105*, 3272–3296.
[87] R. H. Crabtree, G. E. Morris, *J. Organomet. Chem.* **1977**, *135*, 395–403.
[88] R. H. Crabtree, P. C. Demon, D. Eden, J. M. Mihelcic, C. A. Parnell, J. M. Quirk, G. E. Morris, *J. Am. Chem. Soc.* **1982**, *104*, 6994.
[89] A. Macchioni, *Chem. Rev.* **2005**, *105*, 2039–2073.
[90] A. Rifat, N. J. Patmore, M. F. Mahon, A. S. Weller, *Organometallics* **2002**, *21*, 2856–2865.
[91] P. D. W. Boyd, C. A. Reed, *Acc. Chem. Res.* **2005**, *38*, 235–242.
[92] J. van den Broeke, E. de Wolf, B. J. Deelman, G. van Koten, *Adv. Synth. Catal.* **2003**, *345*, 625–634.
[93] A. Lightfoot, P. Schnider, A. Pfaltz, *Angew. Chem.* **1998**, *110*, 3047–3050; *Angew. Chem. Int. Ed.* **1998**, *37*, 2897–2899.
[94] S. P. Smidt, N. Zimmermann, M. Studer, A. Pfaltz, *Chem. Eur. J.* **2004**, *10*, 4685–4693.
[95] R. D. Broene, S. L. Buchwald, *J. Am. Chem. Soc.* **1993**, *115*, 12569–12570.
[96] M. V. Troutman, D. H. Appella, S. L. Buchwald, *J. Am. Chem. Soc.* **1999**, *121*, 4916–4917.
[97] V. P. Conticello, L. Brard, M. A. Giardello, Y. Tsuji, M. Sabat, C. L. Stern, T. J. Marks, *J. Am. Chem. Soc.* **1992**, *114*, 2761–2762.
[98] M. A. Giardello, V. P. Conticello, L. Brard, M. R. Gagne, T. J. Marks, *J. Am. Chem. Soc.* **1994**, *116*, 10241–10254.
[99] D. R. Hou, J. Reibenspies, T. J. Colacot, K. Burgess, *Chem. Eur. J.* **2001**, *7*, 5391–5400.

  

[100] J. Cipot, R. McDonald, M. Stradiotto, *Chem. Commun.* **2005**, 4932–4934.
[101] T. Belser, M. Stohr, A. Pfaltz, *J. Am. Chem. Soc.* **2005**, *127*, 8720–8731.
[102] T. Burgi, A. Baiker, *Acc. Chem. Res.* **2004**, *37*, 909–917.
[103] J. D. Horvath, A. Koritnik, P. Kamakoti, D. S. Sholl, A. J. Gellman, *J. Am. Chem. Soc.* **2004**, *126*, 14988–14994.
[104] J. D. Horvath, A. J. Gellman, *J. Am. Chem. Soc.* **2002**, *124*, 2384–2392.
[105] J. D. Horvath, A. J. Gellman, *J. Am. Chem. Soc.* **2001**, *123*, 7953–7954.
[106] L. F. Liotta, G. Deganello, D. Sannino, M. C. Gaudino, P. Ciambelli, S. Gialanella, *Appl. Catal. A* **2002**, *229*, 217–227.
[107] H. Tanaka, S. I. Ito, S. Kameoka, K. Tomishige, K. Kunimori, *Catal. Commun.* **2003**, *4*, 1–4.
[108] N. Macleod, J. Isaac, R. M. Lambert, *J. Catal.* **2001**, *198*, 128–135.
[109] L. F. Liotta, G. A. Martin, G. Deganello, *J. Catal.* **1996**, *164*, 322–333.
[110] L. F. Liotta, G. Deganello, P. Delichere, C. Leclercq, G. A. Martin, *J. Catal.* **1996**, *164*, 334–340.
[111] A. M. Venezia, A. Rossi, L. F. Liotta, A. Martorana, G. Deganello, *Appl. Catal. A* **1996**, *147*, 81–94.
[112] L. Guczi, *Catal. Today* **2005**, *101*, 53–64.
[113] A. M. Venezia, V. La Parola, B. Pawelec, J. L. G. Fierro, *Appl. Catal. A* **2004**, *264*, 43–51.
[114] A. M. Venezia, L. F. Liotta, G. Pantaleo, V. La Parola, G. Deganello, A. Beck, Z. Koppany, K. Frey, D. Horvath, L. Guczi, *Appl. Catal. A* **2003**, *251*, 359–368.
[115] S. M. Barlow, R. Raval, *Surf. Sci. Rep.* **2003**, *50*, 201–341.
[116] V. Humblot, S. M. Barlow, R. Raval, *Prog. Surf. Sci.* **2004**, *76*, 1–19.
[117] M. Studer, H. U. Blaser, C. Exner, *Adv. Synth. Catal.* **2003**, *345*, 45–65.
[118] C. Exner, A. Pfaltz, M. Studer, H. U. Blaser, *Adv. Synth. Catal.* **2003**, *345*, 1253–1260.
[119] M. von Arx, T. Burgi, T. Mallat, A. Baiker, *Chem. Eur. J.* **2002**, *8*, 1430–1437.
[120] N. Bonalumi, A. Vargas, D. Ferri, T. Burgi, T. Mallat, A. Baiker, *J. Am. Chem. Soc.* **2005**, *127*, 8467–8477.
[121] O. J. Sonderegger, G. M. W. Ho, T. Burgi, A. Baiker, *J. Mol. Catal. A* **2005**, *229*, 19–24.
[122] T. Burgi, A. Baiker, *J. Am. Chem. Soc.* **1998**, *120*, 12920–12926.
[123] A. I. McIntosh, D. J. Watson, J. W. Burton, R. M. Lambert, *J. Am. Chem. Soc.* **2006**, *128*, 7329–7334.
[124] K. Ziegler, Belgian Patent 533362, **1954**.
[125] K. Ziegler, E. Holzkamp, H. Martin, H. Breil, *Angew. Chem.* **1955**, *67*, 541–547.
[126] G. Natta, *J. Polym. Sci.* **1955**, *16*, 143.
[127] G. Natta, *Angew. Chem.* **1956**, *68*, 393.
[128] Y. V. Kissin, *Isospecific polymerization of olefins with heterogeneous Ziegler-Natta Catalysts*, Springer, New York, **1985**.
[129] L. L. Böhm, *Angew. Chem.* **2003**, *115*, 5162–5183; *Angew. Chem. Int. Ed.* **2003**, *42*, 5010–5030.
[130] G. Wilke, *Angew. Chem.* **2003**, *115*, 5150–5159; *Angew. Chem. Int. Ed.* **2003**, *42*, 5000–5008.
[131] J. P. Hogan, *J. Polym. Sci. Part A* **1970**, *8*, 2637–2652.
[132] J. P. Hogan, R. L. Banks, US Patent 2825721, **1958**.
[133] A. Clark, *Catal. Rev.* **1970**, *3*, 145–173.
[134] M. P. McDaniel, *Adv. Catal.* **1985**, *33*, 47–98.
[135] B. M. Weckhuysen, I. E. Wachs, R. A. Shoonheydt, *Chem. Rev.* **1996**, *96*, 3327–3349.
[136] E. Groppo, C. Lamberti, S. Bordiga, G. Spoto, A. Zecchina, *Chem. Rev.* **2005**, *105*, 115–183, and references therein.
[137] H. H. Brintzinger, D. Fischer, R. Mülhaupt, B. Rieger, R. M. Waymouth, *Angew. Chem.* **1995**, *107*, 1255–1283; *Angew. Chem. Int. Ed. Engl.* **1995**, *34*, 1143–1170.
[138] K. H. Theopold, *Eur. J. Inorg. Chem.* **1998**, 15–24.
[139] L. Resconi, L. Cavallo, A. Fait, F. Piemontesi, *Chem. Rev.* **2000**, *100*, 1253–1345.
[140] H. G. Alt, A. Koppl, *Chem. Rev.* **2000**, *100*, 1205–1221.
[141] A. T. Rappe, W. M. Skiff, C. J. Casewit, *Chem. Rev.* **2000**, *100*, 1435–1456.
[142] K. Vanka, Z. Xu, M. Seth, T. Ziegler, *Top. Catal.* **2005**, *34*, 143–164.
[143] M. Boero, M. Parrinello, H. Weiss, S. Huffer, *J. Phys. Chem. A* **2001**, *105*, 5096–5105.
[144] M. Boero, M. Parrinello, K. Terakura, *J. Am. Chem. Soc.* **1998**, *120*, 2746–2752.
[145] G. Monaco, M. Toto, G. Guerra, P. Corradini, L. Cavallo, *Macromolecules* **2000**, *33*, 8953–8962.
[146] E. Puhakka, T. T. Pakkanen, T. A. Pakkanen, *Surf. Sci.* **1995**, *334*, 289–294.
[147] P. Corradini, U. Barone, R. Fusco, G. Guerra, *Gazz. Chim. Ital.* **1983**, *113*, 601.
[148] P. Cossee, *J. Catal.* **1964**, *3*, 80–88.
[149] E. J. Arlman, *J. Catal.* **1964**, *3*, 89–98.
[150] E. J. Arlman, P. Cossee, *J. Catal.* **1964**, *3*, 99–104.
[151] E. Albizzati, U. Giannini, G. Collina, L. Noristi, L. Resconi in *Polypropylene Handbook* (Ed.: E. P. J. Moore), Hanser, München, **1996**.
[152] J. C. Chadwick, *Macromol. Symp.* **2001**, *173*, 21–35.
[153] E. Puhakka, T. T. Pakkanen, T. A. Pakkanen, *J. Phys. Chem. A* **1997**, *101*, 6063–6068.
[154] E. Puhakka, T. T. Pakkanen, T. A. Pakkanen, *J. Mol. Catal. A* **1997**, *123*, 171–178.
[155] J. C. Chadwick, G. Morini, G. Balbontin, I. Mingozzi, E. Albizzati, O. Sudmeijer, *Macromol. Chem. Phys.* **1997**, *198*, 1181–1188.
[156] J. C. Chadwick, G. M. M. Vankessel, O. Sudmeijer, *Macromol. Chem. Phys.* **1995**, *196*, 1431–1437.
[157] J. C. Chadwick, A. Miedema, O. Sudmeijer, *Macromol. Chem. Phys.* **1994**, *195*, 167–172.
[158] V. Busico, R. Cipullo, G. Talarico, A. L. Segre, J. C. Chadwick, *Macromolecules* **1997**, *30*, 4786–4790.
[159] K. H. Theopold, *Chemtech* **1997**, *27*, 26–32.
[160] B. M. Weckhuysen, R. A. Schoonheydt, *Catal. Today* **1999**, *51*, 215–221.
[161] A. Zecchina, E. Garrone, G. Ghiotti, S. Coluccia, *J. Phys. Chem.* **1975**, *79*, 972–978.
[162] A. Zecchina, E. Garrone, G. Ghiotti, C. Morterra, E. Borello, *J. Phys. Chem.* **1975**, *79*, 966–972.
[163] A. Zecchina, D. Scarano, S. Bordiga, G. Spoto, C. Lamberti, *Adv. Catal.* **2001**, *46*, 265–397.
[164] E. Groppo, C. Lamberti, F. Cesano, A. Zecchina, *Phys. Chem. Chem. Phys.* **2006**, *8*, 2453–2456.
[165] E. Groppo, C. Lamberti, S. Bordiga, G. Spoto, A. Zecchina, *J. Catal.* **2006**, *240*, 172–181.
[166] G. Ghiotti, E. Garrone, G. Della Gatta, B. Fubini, E. Giamello, *J. Catal.* **1983**, *80*, 249–262.
[167] G. Ghiotti, E. Garrone, A. Zecchina, *J. Mol. Catal.* **1988**, *46*, 61–77.
[168] G. Ghiotti, E. Garrone, A. Zecchina, *J. Mol. Catal.* **1991**, *65*, 73–83.
[169] A. Zecchina, G. Spoto, G. Ghiotti, E. Garrone, *J. Mol. Catal.* **1994**, *86*, 423–446.
[170] S. Bordiga, S. Bertarione, A. Damin, C. Prestipino, G. Spoto, C. Lamberti, A. Zecchina, *J. Mol. Catal. A* **2003**, *204*, 527–534.
[171] E. Groppo, C. Lamberti, S. Bordiga, G. Spoto, A. Zecchina, *J. Phys. Chem. B* **2005**, *109*, 15024–15031.
[172] E. Groppo, C. Lamberti, G. Spoto, S. Bordiga, G. Magnacca, A. Zecchina, *J. Catal.* **2005**, *236*, 233–244.
[173] E. Y. X. Chen, T. J. Marks, *Chem. Rev.* **2000**, *100*, 1391–1434.
[174] A. Correa, L. Cavallo, *J. Am. Chem. Soc.* **2006**, *128*, 10952–10959.
[175] A. L. McKnight, R. M. Waymouth, *Chem. Rev.* **1998**, *98*, 2587–2598.
[176] T. J. M. de Bruin, L. Magna, P. Raybaud, H. Toulhoat, *Organometallics* **2003**, *22*, 3404–3413.
[177] A. N. J. Blok, P. H. M. Budzelaar, A. W. Gal, *Organometallics* **2003**, *22*, 2564–2570.

  

[178] S. Tobisch, T. Ziegler, *J. Am. Chem. Soc.* **2004**, *126*, 9059–9071.
[179] G. Guerra, P. Longo, L. Cavallo, P. Corradini, L. Resconi, *J. Am. Chem. Soc.* **1997**, *119*, 4394–4403.
[180] V. Busico, R. Cipullo, G. Talarico, A. L. Segre, L. Caporaso, *Macromolecules* **1998**, *31*, 8720–8724.
[181] M. Dahlmann, G. Erker, M. Nissinen, R. Frohlich, *J. Am. Chem. Soc.* **1999**, *121*, 2820–2828.
[182] V. Busico, R. Cipullo, F. Cutillo, M. Vacatello, *Macromolecules* **2002**, *35*, 349–354.
[183] R. Mülhaupt, *Macromol. Chem. Phys.* **2003**, *204*, 289–327.
[184] K. Beckerle, C. Capacchione, H. Ebeling, R. Manivannan, R. Mülhaupt, A. Proto, T. P. Spaniol, J. Okuda, *J. Organomet. Chem.* **2004**, *689*, 4636–4641.
[185] M. Bochmann, *J. Organomet. Chem.* **2004**, *689*, 3982–3998.
[186] J. A. Ewen, *J. Am. Chem. Soc.* **1984**, *106*, 6355–6364.
[187] J. A. Ewen, *J. Am. Chem. Soc.* **1988**, *110*, 6255.
[188] P. L. Bryant, C. R. Harwell, A. A. Mrse, E. F. Emery, Z. H. Gan, T. Caldwell, A. P. Reyes, P. Kuhns, D. W. Hoyt, L. S. Simeral, R. W. Hall, L. G. Butler, *J. Am. Chem. Soc.* **2001**, *123*, 12009–12017.
[189] E. Zurek, T. Ziegler, *Prog. Polym. Sci.* **2004**, *29*, 107–148, and references therein.
[190] "Modeling methylaluminoxane (MAO)": E. Zurek, T. K. Woo, T. K. Firman, T. Ziegler in *Organometallic catalysts and olefin polymerization* (Eds.: R. Blom, A. Follestad, E. Rytter, M. Tilset, M. Ystenes), Springer, Berlin, **2001**, p. 109–123.
[191] "Structures of MAO: experimental data and molecular models according to DFT quantum-chemical simulations": V. A. Zakharov, I. I. Zakharov, V. N. Panchenko in *Organometallic catalysts and olefin polymerization* (Eds.: R. Blom, A. Follestad, E. Rytter, M. Tilset, M. Ystenes), Springer, Berlin, **2001**, p. 109–123.
[192] H. Sinn, W. Kaminsky, H.-J. Vollmer, R. Woldt, *Angew. Chem.* **1980**, *92*, 396–402; *Angew. Chem. Int. Ed. Engl.* **1980**, *19*, 390–392.
[193] I. I. Zakharov, V. A. Zakharov, *Macromol. Theory Simul.* **2001**, *10*, 108–116.
[194] C. J. Harlan, M. R. Mason, A. R. Barron, *Organometallics* **1994**, *13*, 2957–2969.
[195] M. R. Mason, J. M. Smith, S. G. Bott, A. R. Barron, *J. Am. Chem. Soc.* **1993**, *115*, 4971–4984.
[196] P. A. Deck, C. L. Beswick, T. J. Marks, *J. Am. Chem. Soc.* **1998**, *120*, 1772–1784.
[197] E. Zurek, T. Ziegler, *Faraday Discuss.* **2003**, *124*, 93–109.

Published online: February 12, 2007

  